Supporting Information:

Boosting Sulfides Photooxidation by Fusing Naphthalimide and Flavin together

Huimin Guo†,*, Zhiwen Lei†, Xiaolin Ma†, Siyu Liu†, Yang Qiu†, Jianzhang Zhao†

† State Key Laboratory of Fine Chemicals, Department of Chemistry, Dalian University of Technology, No. 2, Linggong Road, Dalian, 116024, P. R. China.

Contents

This file includes 54 figures and 3 Tables within 32 pages.

KEYWORDS: Photophysics; Flavin; Photocatalysis; Photooxidation; Intersystem Crossing; Internal Conversion

* Corresponding authors, email: guohm@dlut.edu.cn (H. G.)

1 General Information

All the chemicals used in synthesis were of analytical purity and were used as received. Solvents were dried and distilled before used for synthesis.

Analytical Measurements. All chemicals are analytically pure and used as received. NMR spectra were recorded on a Bruker 400 MHz spectrometer and Bruker 500 MHz spectrometer with CDCl3, DMSO-d6 as solvents and tetramethylsilane (TMS) as standard at 0.00 ppm. HRMS were measured with a G6224A (Aglient, U.S.).

Spectroscopic Measurements. Absorption spectrum were recorded on an UV2550 UV−Vis spectrophotometer (Shimadzu, Japan). Fluorescence spectra were measured on an FS5 spectrophotometer (Edinburgh Instruments, UK). Fluorescence lifetimes were measured with an OB920 luminescence lifetime spectrometer (Edinburgh Instruments, UK). The nanosecond transient absorption spectra were measured on LP920 laser flash photolysis spectrometer (Edinburgh Instruments, UK). Luminescence Quantum Yield were measured with an C13534-11 Quantaurus-QY Plus (Hamamatsu Photonics, Japan).

Preparation of Sample Solution for Spectroscopic Measurements. The compound was dissolved in a small amount of solvent in a 5 mL volumetric flask and then toluene was added to get 5 mL solution (1.0×10^{-3} M).

Measurement of Singlet Oxygen Quantum Yield (Φ_Δ).

The excited photosensitizer reacts with O_2 to produce singlet oxygen ($^1O_2$). 1,3-Diphenylisobenzofuran (DPBF) was used as $^1O_2$ scavenger and the $^1O_2$ produced was monitored by absorbance of DPBF at 414 nm. Xenon lamp (350 nm) was used

for measurement of Φ_Δ. In measurements, DPBF was firstly dissolved to make a solution. A certain volume of this DPBF solution was used to make a 3 mL solution and the absorbance at 414 nm was normalized to 1. Then, the same amount of DPBF solution was used in the whole measurement. The dosage of photosensitizer was determined by the absorbance at 350 nm. The amount of photosensitizers (unknown sample or standard $[Ru(Bpy)_3]^{2+}$) used was adjusted according to the absorbance at 350 nm (A_{unk} or A_{std}), so that the solutions of the unknown sample and the standard should give the same absorbance at 350 nm. To yield reasonable results, the absorbance of sample and standard should be 0.2~0.3 L×mol^{-1}×cm^{-1}. Then, DPBF was added and the absorbance was measured with respect to radiation time. According to the UV-Vis absorption spectra of the sample after adding DPBF, the slopes (m_{unk} or m_{std}) of the absorbance of DPBF changing over time at 414 nm can be obtained. The Φ_Δ of the sample can be calculated according to Eq. 1.

$$\Phi_{\Delta,unk} = \Phi_{\Delta,std}(\frac{A_{std}}{A_{unk}})(\frac{m_{unk}}{m_{std}})(\frac{\eta_{unk}}{\eta_{std}})^2 \qquad (Eq.\ 1)$$

In Eq. 1, unk and std indicate the unknown sample and the standard, respectively. Φ_Δ, *A*, *m*, and *η* represent singlet oxygen quantum yield, absorbance of sample/standard in solution without DPBF at excitation wavelength (350 nm), slope of the change of absorbance of sample/standard + DPBF mixtures with time, and refractive index of the solvent used for measurement, respectively. As change of absorbance with respect to time were used in calculation of absolute values of the slopes, the absorbance of samples at 414 nm were not subtracted considering the absorbance of a sample is constant at steady state. $[Ru(bpy)_3]^{2+}$ was used as standard ($\Phi_\Delta = 0.57$ in DCM).[1-4]

2 Synthesis and Molecular Structure Characterization Data
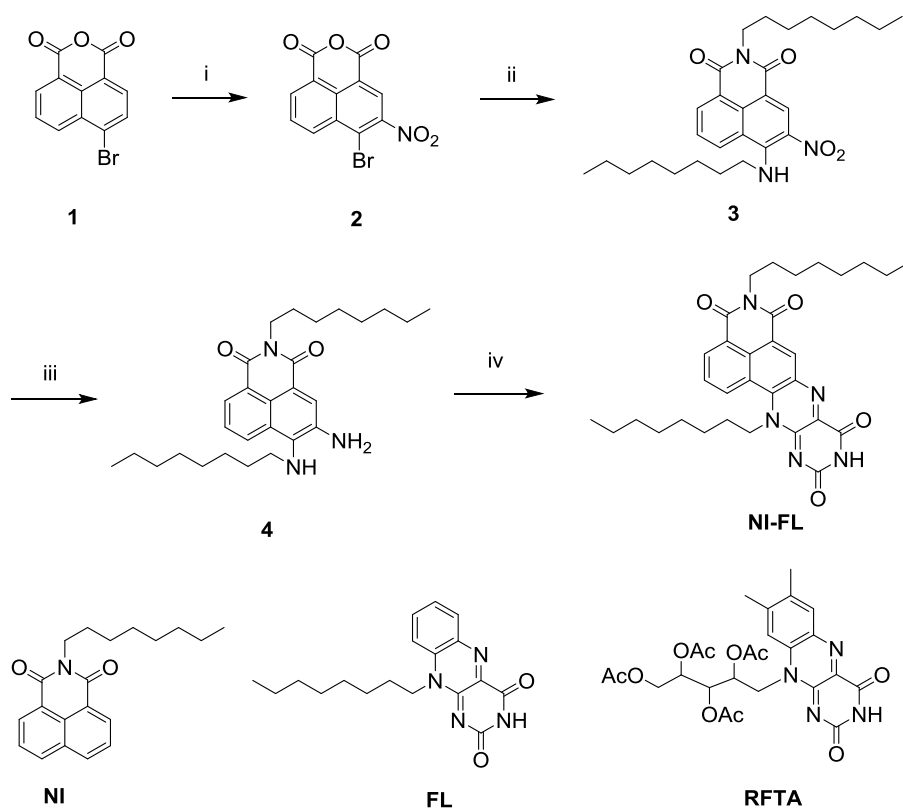
Scheme S1. Synthesis of the compounds. (i) H_2SO_4, $NaNO_3$, 0 °C, 3 h ;(ii) n-octylamine, Et_3N, THF, 66 °C, 3 h ; (iii) $SnCl_2$, concentrated hydrochloric acid, ethanol, refluxed, 3 h; (iv) Alloxan, boric acid, acetic acid glacial, 60 °C, 3 h.

Synthesis of the compound 2: Sodium nitrate (2.0 g, 23.4 mmol) was carefully added to 4-bromo-1,8-naphthalic anhydride (5.0 g, 18 mmol) in concentrated sulfuric acid (20 mL) , keeping the temperature at 0 °C . After stirred for 3 h at 0 °C and another 1 h in room temperature, the solution was poured into water and ice. The precipitate formed was filtered, washed with water and dried to obtain compound **2** (4.3 g). Yellow solid, yield: 74.8 %. ^{1}H NMR (500 MHz, $CDCl_3$): δ (ppm) 8.92 (m, 1H), 8.84 (m, 1H), 8.82 (s, 1H), 8.10 (m, 1H).

Synthesis of the compound 3: n- octylamine (3.6 mL, 18 mmol) and triethylamine (0.9 mL) were dissolved in a solution of compound 2 (966 mg, 3.0 mmol) in THF (60 mL) under nitrogen. After stirred for 3 h at 66 ℃, the solution was concentrated in vacuum and purified by column chromatography (silica gel; CH_2Cl_2 : Petroleum ether = 1: 1, v/v) to obtain compound 3 (1.3 g). Orange solid, yield: 87.5%. ^{1}H NMR (400MHz ,CDCl$_3$): δ (ppm) 9.89 (br. s., 1 H), 9.32 - 9.26 (m, 1 H), 8.71 - 8.61 (m, 2 H), 7.66 - 7.70 (m, 8.4 Hz, 1 H), 4.18 - 4.09 (m, 2 H), 3.94 – 3.97 (m, 2 H), 1.81 - 1.88 (m, 2 H), 1.75 - 1.65 (m, 2 H), 1.50 - 1.23 (m, 20 H), 0.93 - 0.80 (m, 6 H). ESI−TOF−HRMS ([$C_{28}H_{39}N_3O_4$-H]⁻): calcd. 480.2868; found 480.2865.

Synthesis of the compound NI-FL: Compound **3** (442 mg, 0.92 mmol) and SnCl$_2$ (1.7 g, 7.34 mmol) were added to the solution of concentrated hydrochloric acid (5.0 mL) and ethanol (5.0 mL) under nitrogen. After refluxed under nitrogen for 3 h, The reaction mixture was allowed to cool to room temperature and then stirred overnight. The reaction mixture was poured into water and ice and the solution adjusted to pH11 with 5 M NaOH. The Organic layer was washed with water, dried over Na$_2$SO$_4$, filtered, and evaporated to give the compound **4** (354 mg) as a dark yellow solid. To the solution of compound **4** (354 mg) in glacial acetic, alloxan monohydrate (144 mg) and boric acid (80 mg) were added under nitrogen. After stirred for 3 h at 60 ℃, The reaction mixture was concentrated in vacuum and purified by column chromatography (silica gel; CH_2Cl_2 : MeOH = 40: 1, v/v) to obtain compound **NI-FL**(88 mg). Orange solid, yield: 17.2 %. ^{1}H NMR (400 MHz, CDCl$_3$): δ (ppm) 9.51 (dd, J = 0.9, 8.4 Hz, 1

H), 8.79 (s, 1 H), 8.77 - 8.67 (m, 2 H), 8.15 - 8.05 (m, 1 H), 4.92 (br. s., 2 H), 4.27 -

4.14 (m, 2 H), 1.96 (quin, J = 7.8 Hz, 2 H), 1.76 (quin, J = 7.5 Hz, 2 H), 1.62 - 1.26

(m, 20 H), 0.95 - 0.81 (m, 6 H). ESI−TOF−HRMS ([C$_{32}$H$_{39}$N$_{5}$O$_{4}$+H]$^{+}$):

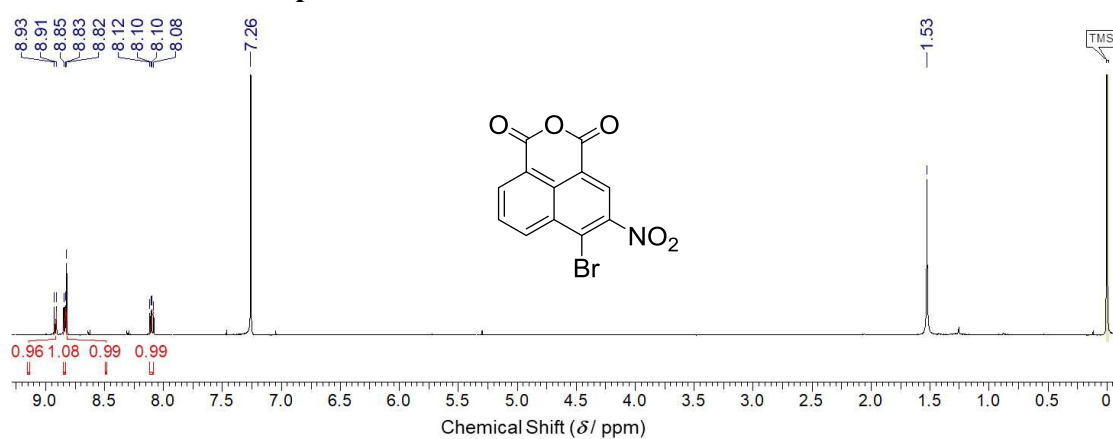calcd.558.3075; found 558.3072.

3 NMR and HRMS spectra

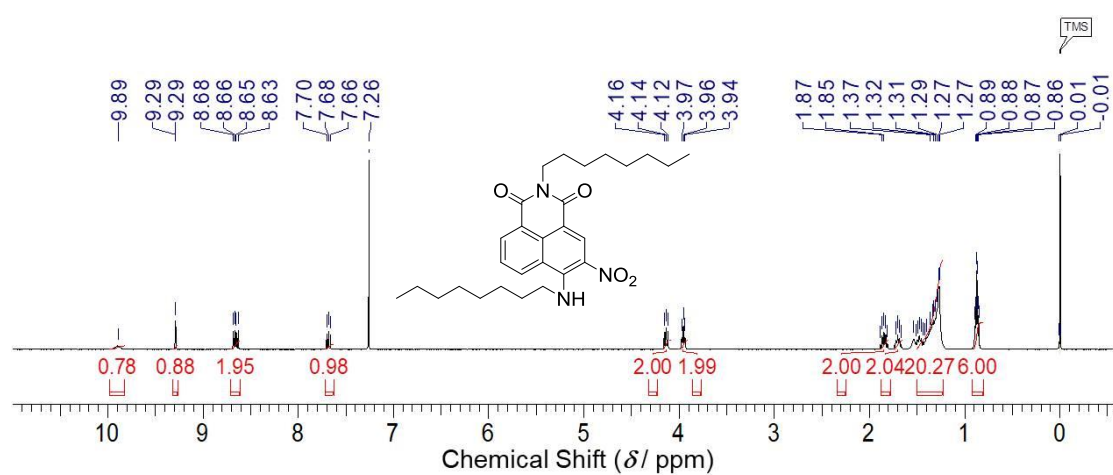**Figure S1.** ^{1}H NMR spectrum of **2** (500 MHz, CDCl$_3$), 25 °C.
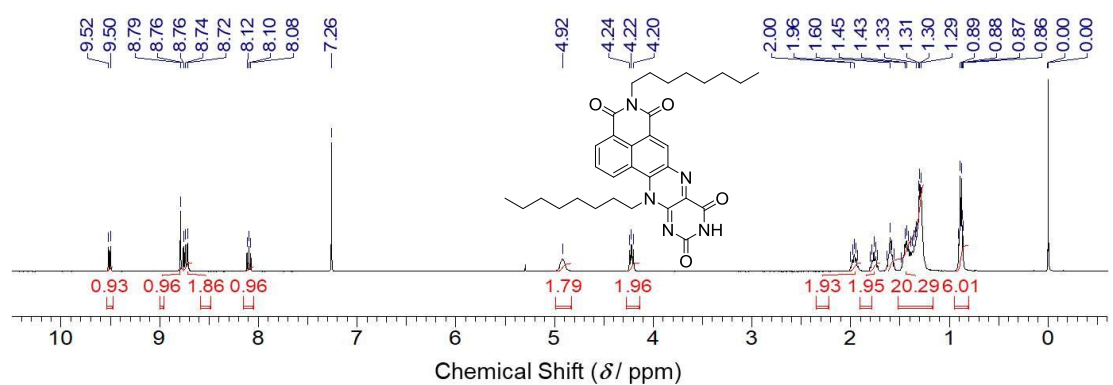

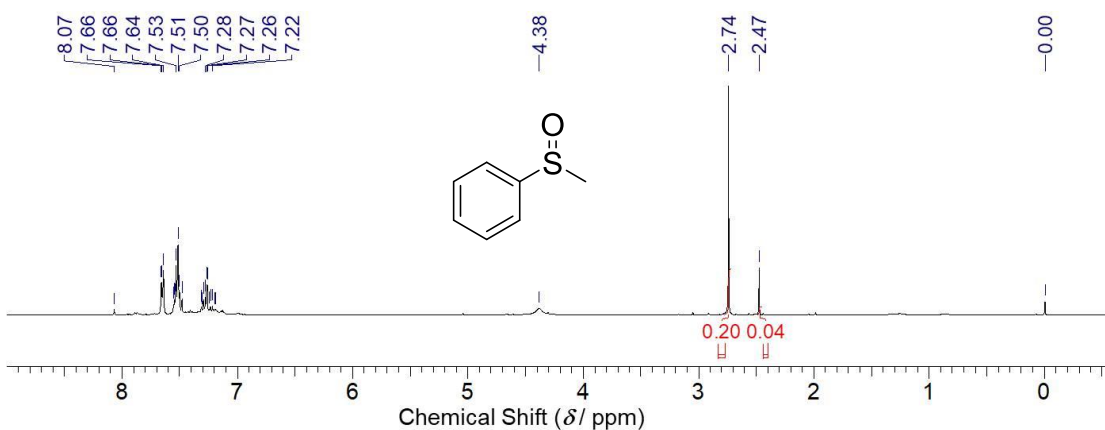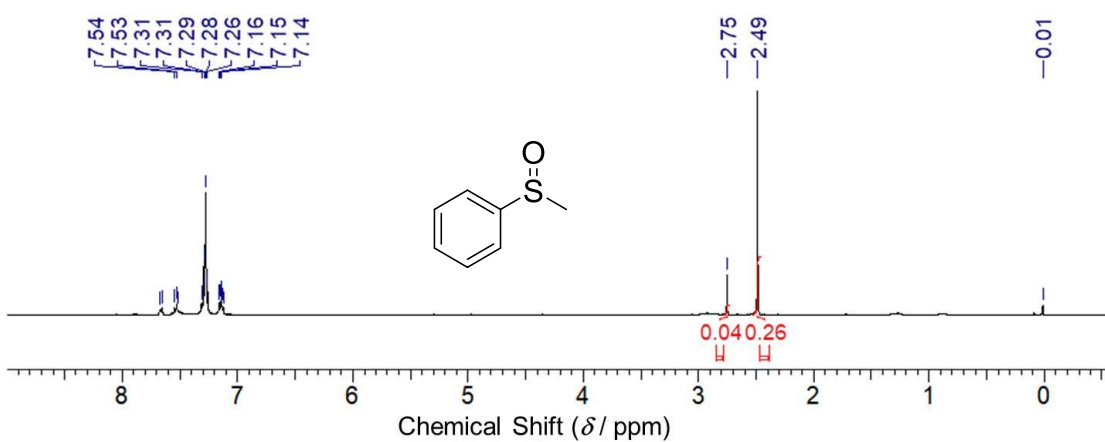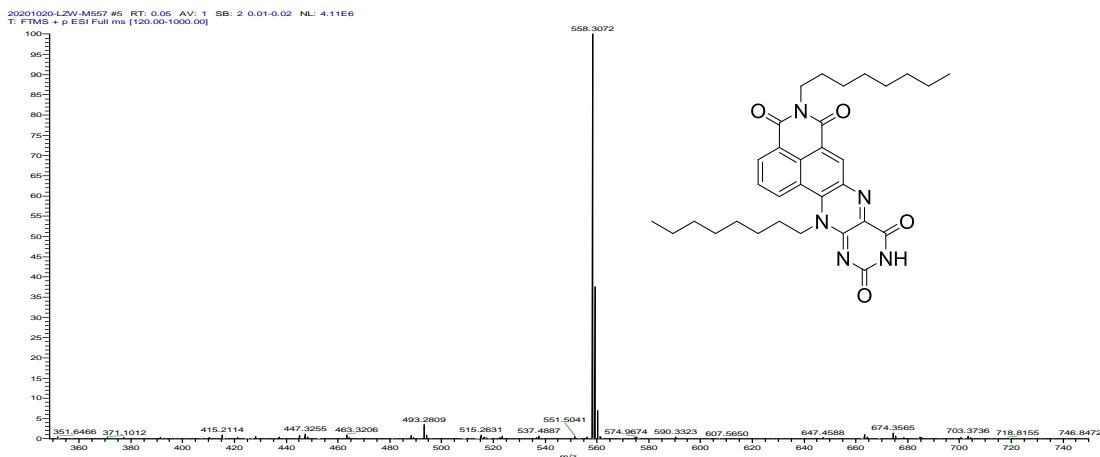**Figure S2.** ^{1}H NMR spectrum of **3** (400 MHz, CDCl$_3$), 25 °C.

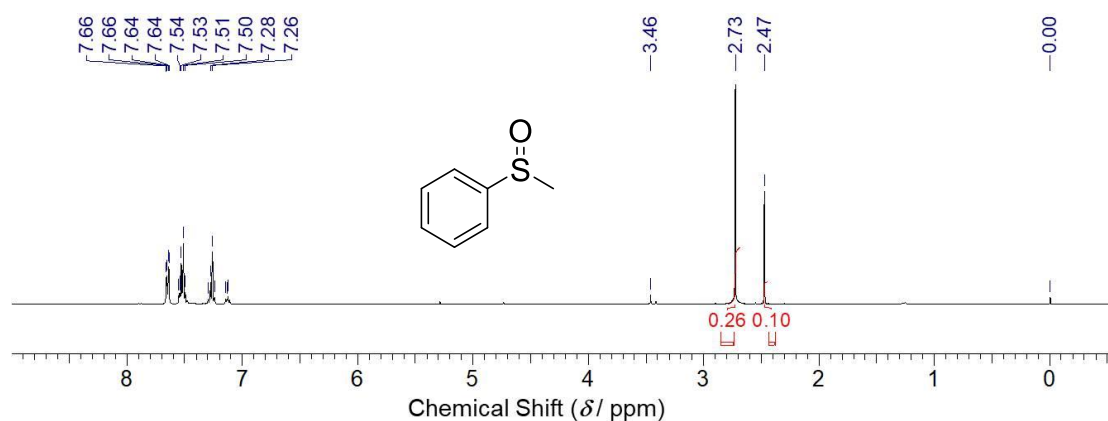**Figure S3.** ^{1}H NMR spectrum of **NI-FL** (400 MHz, CDCl$_3$), 25 °C.
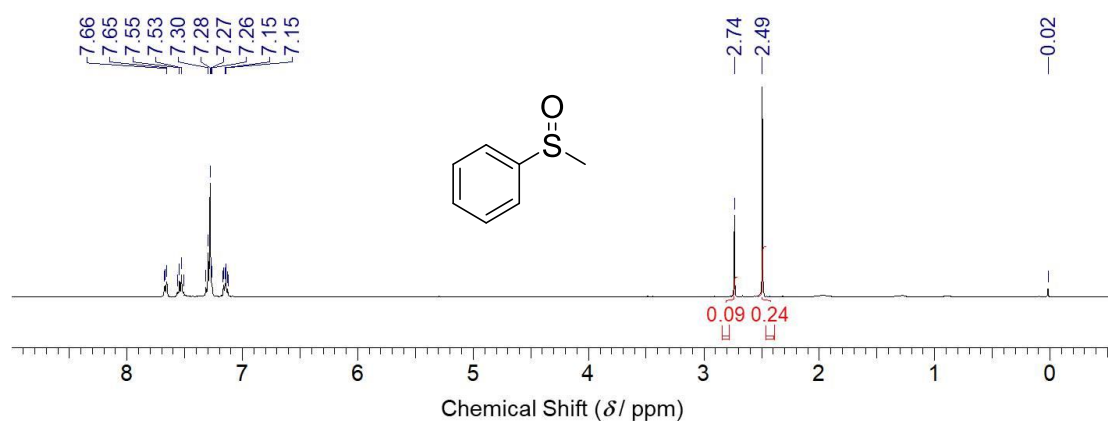
Figure S4. ESI-TOF-HRMS spectrum of **NI-FL**.

Figure S5. ^{1}H NMR (400Hz, CDCl$_3$). **NI-FL** (0.5 mol %) as photocatalyst, in DCM, reaction time 9 h. Yield: 13 %.

Figure S6. ^{1}H NMR (400Hz, CDCl$_3$). **NI-FL** (0.5 mol %) as photocatalyst, in MeCN, reaction time 9 h. Yield: 83 %.

Figure S7. ^{1}H NMR (400Hz, CDCl$_3$). **NI-FL** (0.5 mol %) as photocatalyst, in MeOH, reaction time 9 h. Yield: 72 %.

Figure S8. ^{1}H NMR (400Hz, CDCl$_3$). **NI-FL** (0.5 mol %) as photocatalyst, in DCM/MeOH 9:1 mixture, reaction time 9 h. Yield: 27 %.
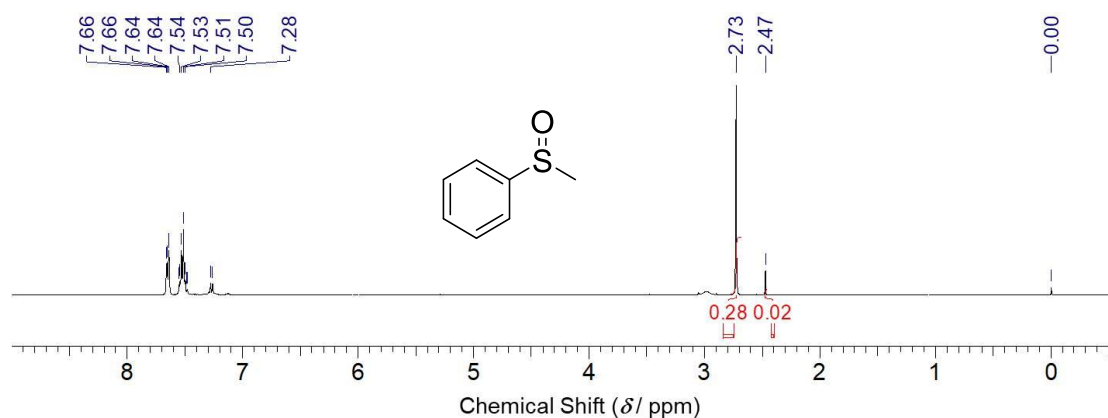

Figure S9. ^{1}H NMR (400Hz, CDCl$_3$). **NI-FL** (0.5 mol %) as photocatalyst, in MeCN/MeOH 9:1 mixture, reaction time 9 h. Yield: 93 %.
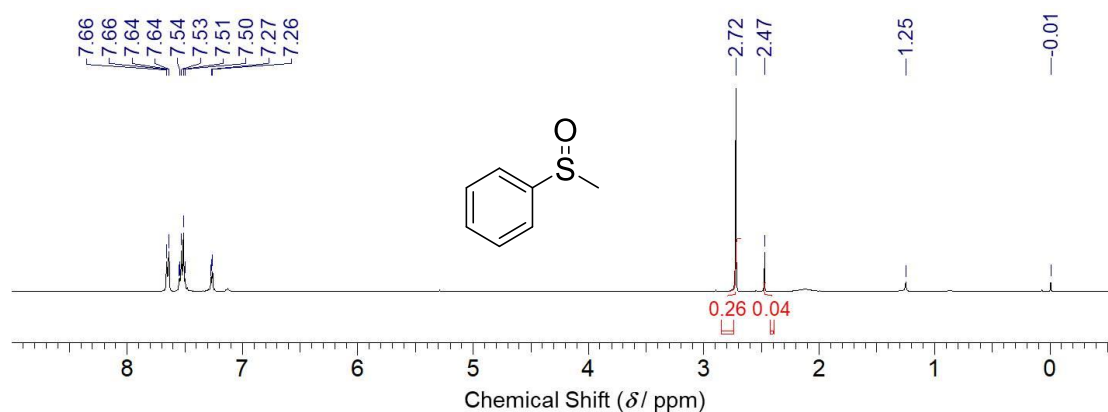
Figure S10. ^{1}H NMR (400Hz, CDCl$_3$). **NI-FL** (0.5 mol %) as photocatalyst, in MeCN/H$_2$O 9:1 mixture, reaction time 9 h. Yield: 87 %.
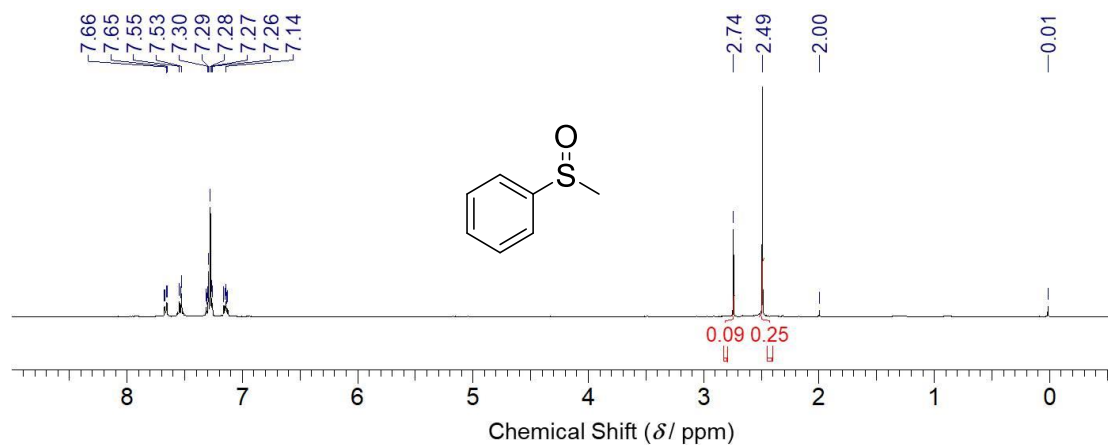

Figure S11. ^{1}H NMR (400Hz, CDCl$_3$). **NI-FL** (0.2 mol %) as photocatalyst, in MeCN/MeOH 9:1 mixture, reaction time 5 h. Yield: 27 %.
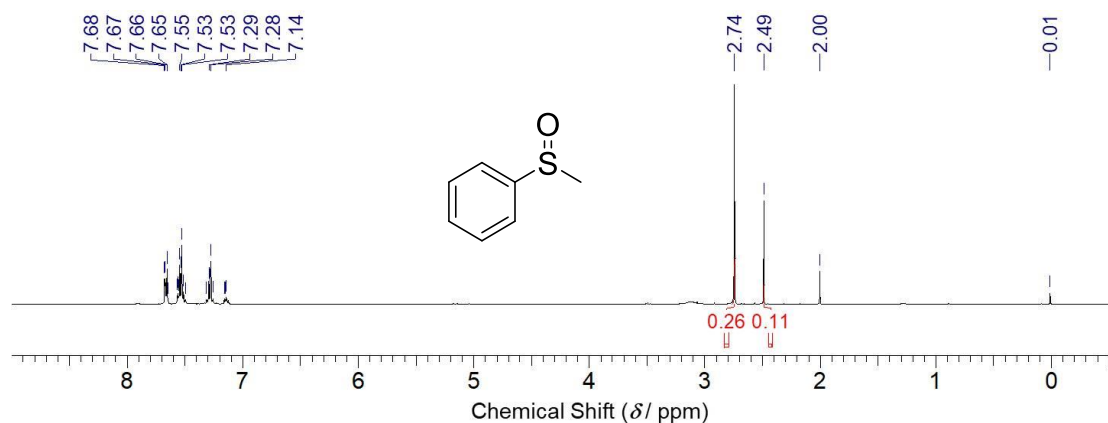

Figure S12. ^{1}H NMR (400Hz, CDCl$_3$). **NI-FL** (0.5 mol %) as photocatalyst, in MeCN/MeOH 9:1 mixture, reaction time 5 h.Yield: 70 %.
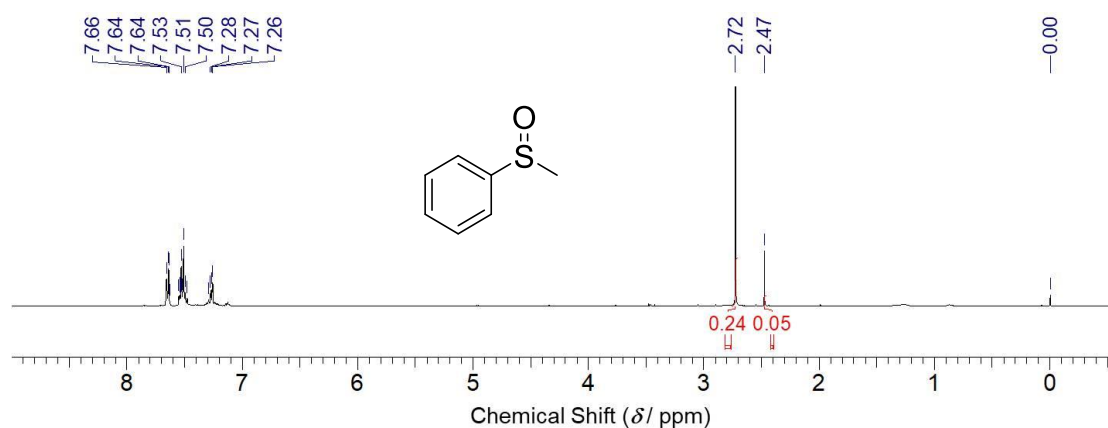
Figure S13. ^{1}H NMR (400Hz, CDCl$_3$). **NI-FL** (1 mol %) as photocatalyst, in MeCN/MeOH 9:1 mixture, reaction time 5 h. Yield: 83 %.
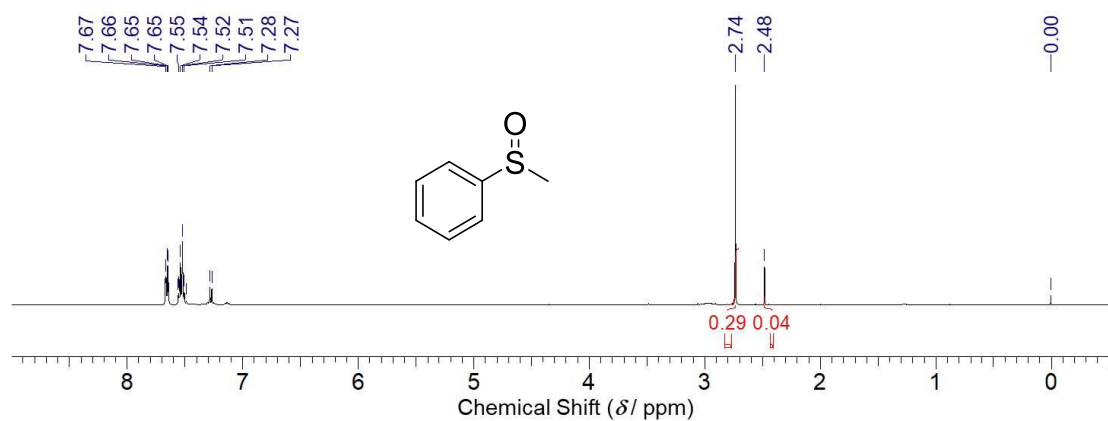

Figure S14. ^{1}H NMR (400Hz, CDCl$_3$). **NI-FL** (2 mol %) as photocatalyst, in MeCN/MeOH 9:1 mixture, reaction time 5 h. Yield: 88 %.
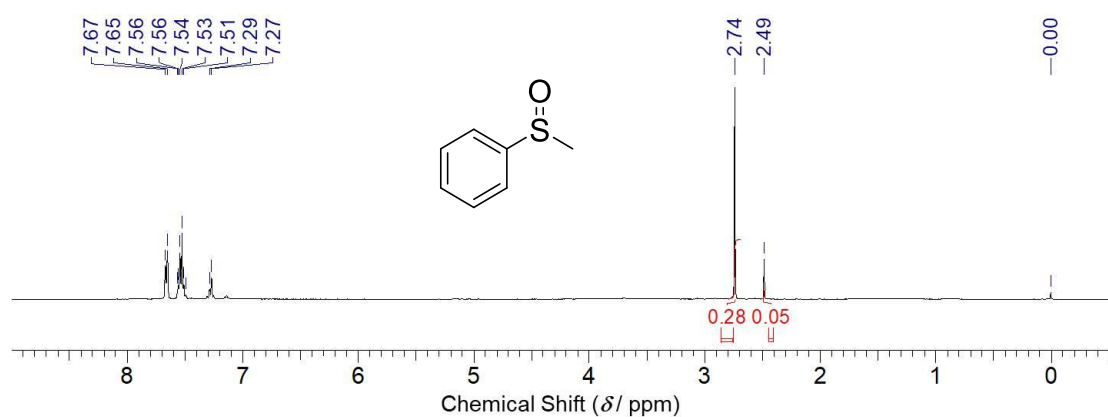

Figure S15. ^{1}H NMR (400Hz, CDCl$_3$). **NI-FL** (0.5 mol %) as photocatalyst, in MeCN/MeOH 9:1 mixture, reaction time 7 h. Yield: 85 %.

Figure S16. ^{1}H NMR (400Hz, CDCl$_3$). **NI-FL** (0.5 mol %) as photocatalyst, in MeCN/MeOH 9:1 mixture, reaction time 9 h, no light. Yield: 0 %.

Figure S17. ^{1}H NMR (400Hz, CDCl$_3$).No **NI-FL** (0.5 mol %) as photocatalyst, in MeCN/MeOH 9:1 mixture, reaction time 9 h. Yield: 0 %.
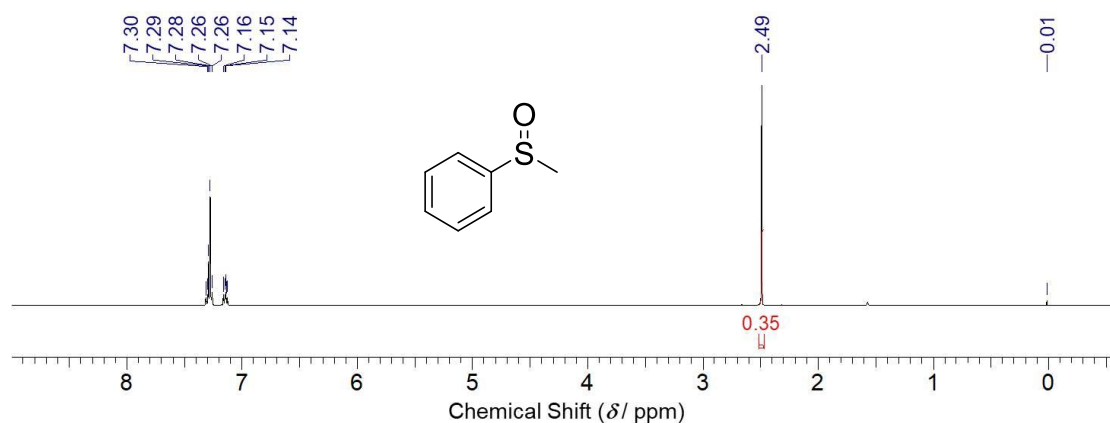

Figure S18. ^{1}H NMR (400Hz, CDCl$_3$).No **NI-FL** (0.5 mol %) as photocatalyst, in MeCN/MeOH 9:1 mixture, reaction time 9 h, no light. Yield: 0 %.
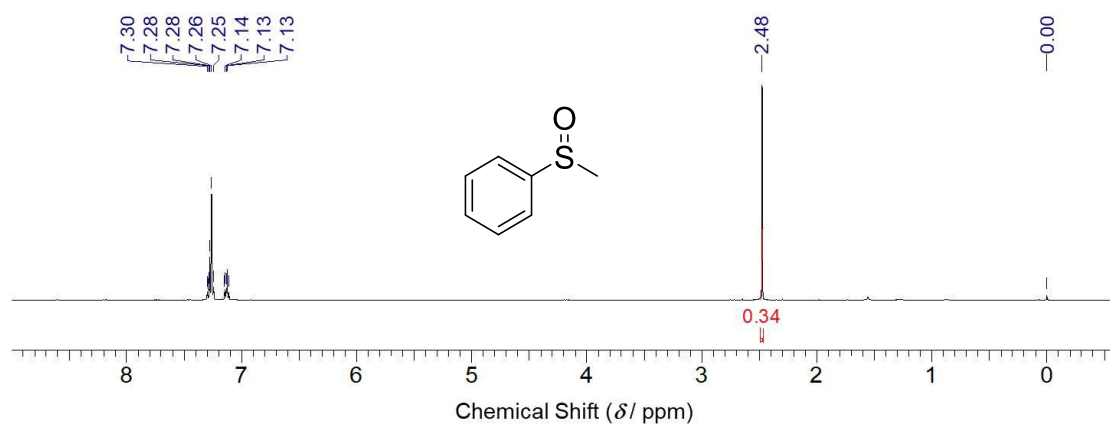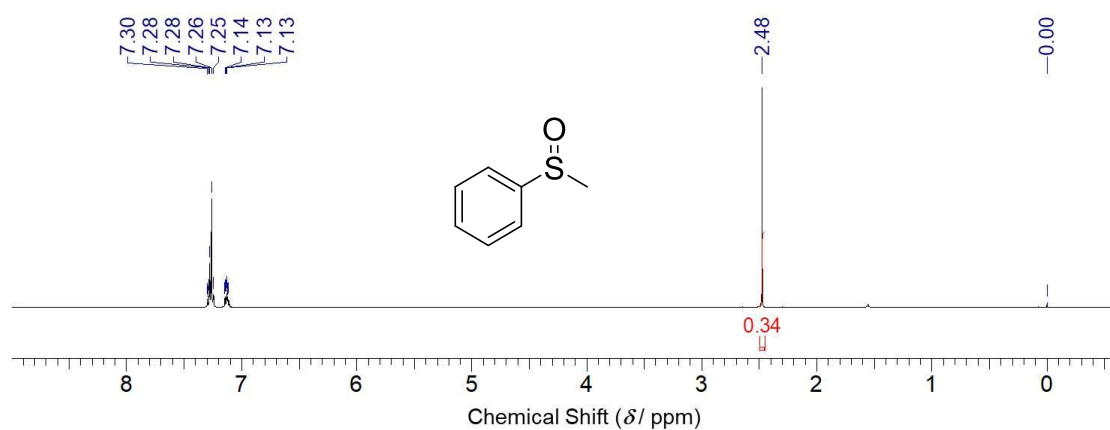
Figure S19. ^{1}H NMR (400Hz, CDCl$_3$). **RFTA** (0.5 mol %) as photocatalyst, in MeCN/MeOH 9:1 mixture, reaction time 7 h. Yield: 29 %.

Figure S20. ^{1}H NMR (400Hz, CDCl$_3$). **FL** (0.5 mol %) as photocatalyst, in MeCN/MeOH 9:1 mixture, reaction time 7 h. Yield: 26 %.

Figure S21. ^{1}H NMR (400Hz, CDCl$_3$). **RFTA** (0.5 mol %) as photocatalyst, in MeCN/MeOH 9:1 mixture, reaction time 9 h. Yield: 59 %.

Figure S22. ^{1}H NMR (400Hz, CDCl$_3$). **FL** (0.5 mol %) as photocatalyst, in MeCN/MeOH 9:1 mixture, reaction time 9 h. Yield: 36 %.

Figure S23. ^{1}H NMR (400Hz, CDCl$_3$). **NI** (0.5 mol %) as photocatalyst, in MeCN/MeOH 9:1 mixture, reaction time 9 h. Yield: 0 %.

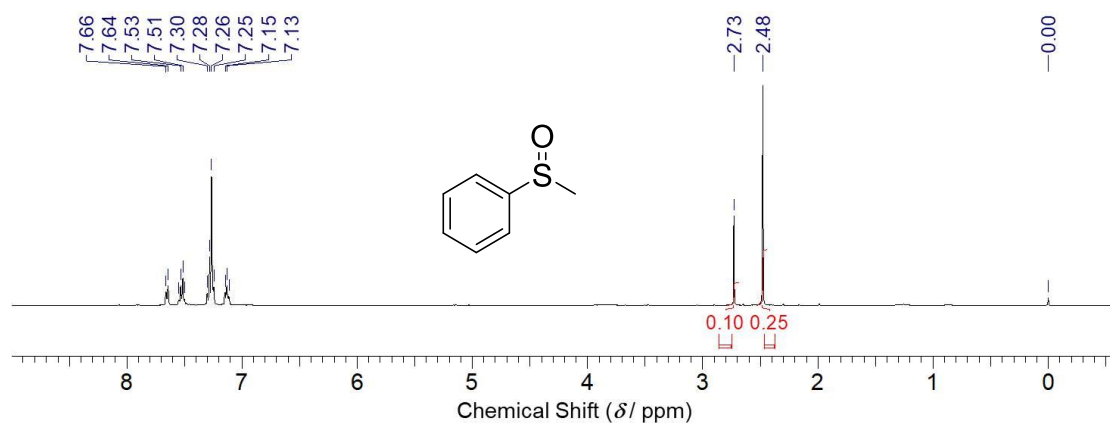**Figure S24.** ^{1}H NMR (400Hz, CDCl$_3$). **NI-FL** (0.5 mol %) as photocatalyst, in MeCN/MeOH 9:1 mixture, reaction time 7 h 30 min. Yield: 72 %.

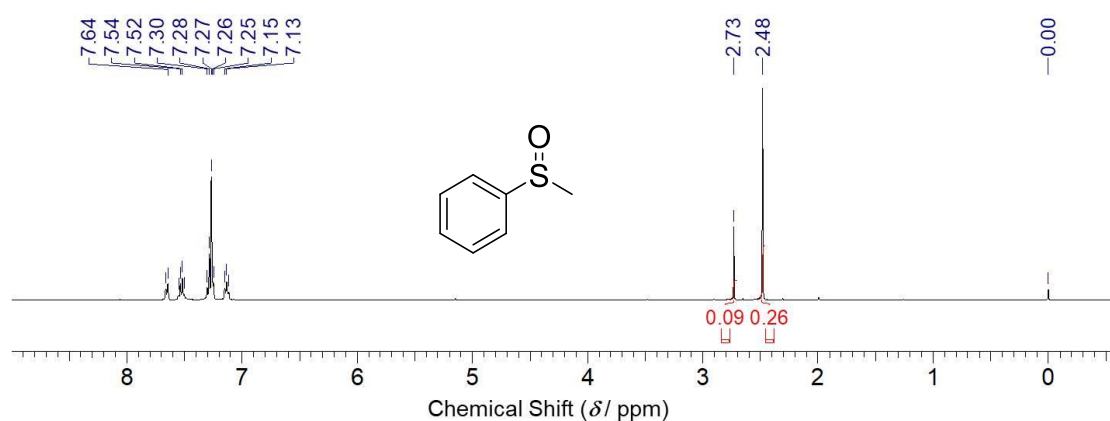**Figure S25.** ^{1}H NMR (400Hz, CDCl$_3$). **RFTA** (0.5 mol %) as photocatalyst, in MeCN/MeOH 9:1 mixture, reaction time 7 h 30 min. Yield: 30 %.

Figure S26. ^{1}H NMR (400Hz, CDCl$_3$). **FL** (0.5 mol %) as photocatalyst, in MeCN/MeOH 9:1 mixture, reaction time 7 h 30 min. Yield: 27 %.

Figure S27. ^{1}H NMR (400Hz, CDCl$_3$). **NI** (0.5 mol %) as photocatalyst, in MeCN/MeOH 9:1 mixture, reaction time 7 h 30 min. Yield: 0 %.

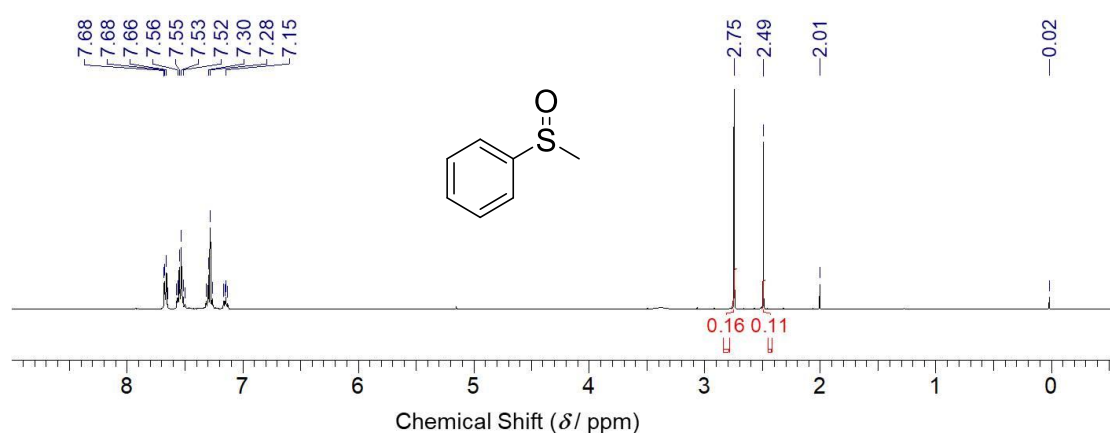**Figure S28.** ^{1}H NMR (400Hz, CDCl$_3$). **NI-FL** (0.5 mol %) as photocatalyst, in MeCN/MeOH 9:1 mixture, reaction time 7 h 10 min. Yield: 64 %.

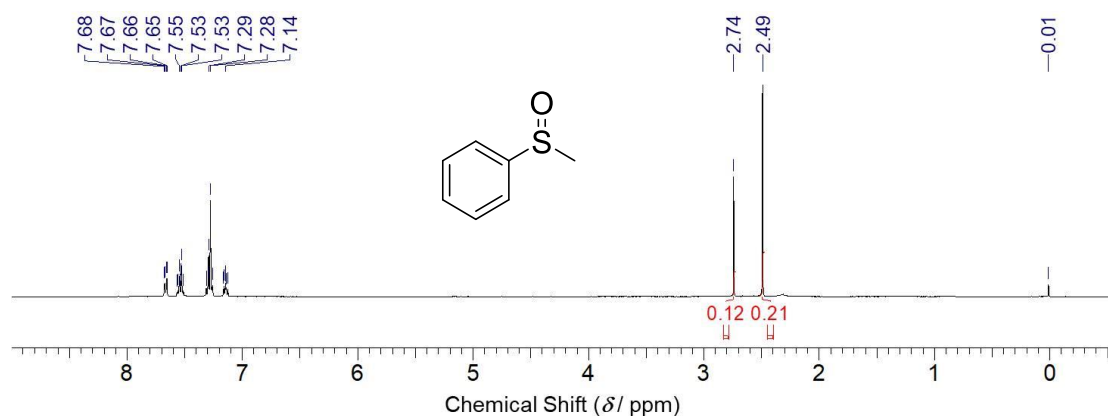**Figure S29.** ^{1}H NMR (400Hz, CDCl$_3$). **RFTA** (0.5 mol %) as photocatalyst, in MeCN/MeOH 9:1 mixture, reaction time 7 h 10 min. Yield: 35 %.

Figure S30. ^{1}H NMR (400Hz, CDCl$_3$). **FL** (0.5 mol %) as photocatalyst, in MeCN/MeOH 9:1 mixture, reaction time 7 h 10 min. Yield: 25 %.
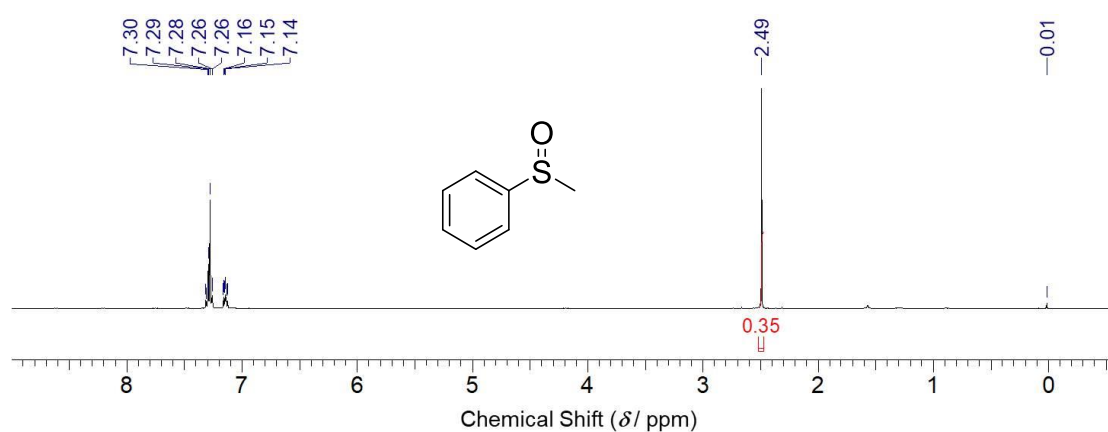
Figure S31. ^{1}H NMR (400Hz, CDCl$_3$). **NI** (0.5 mol %) as photocatalyst, in MeCN/MeOH 9:1 mixture, reaction time 7 h 10 min. Yield: 0 %.
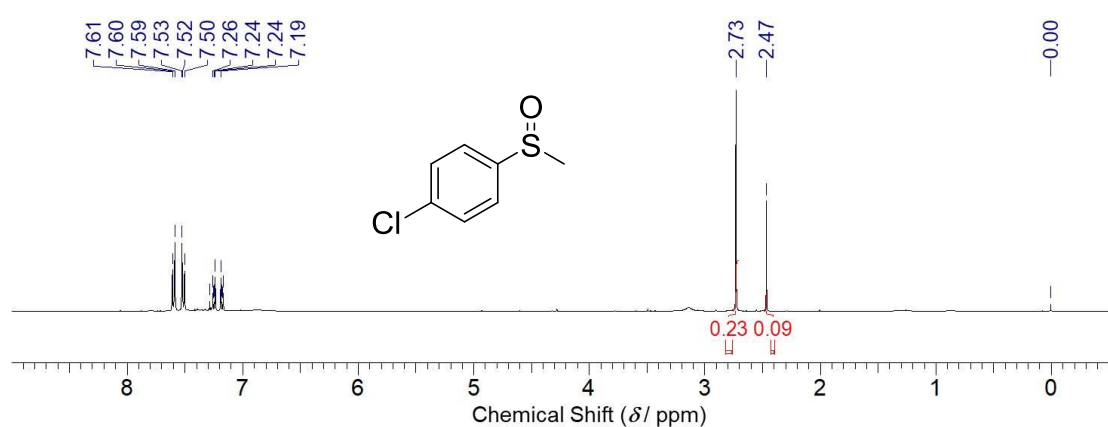

Figure S32. ^{1}H NMR (400Hz, CDCl$_3$). **NI-FL** (0.5 mol %) as photocatalyst, in MeCN/MeOH 9:1 mixture, reaction time 6 h 25 min. Yield: 0 %. Yield: 89 %.
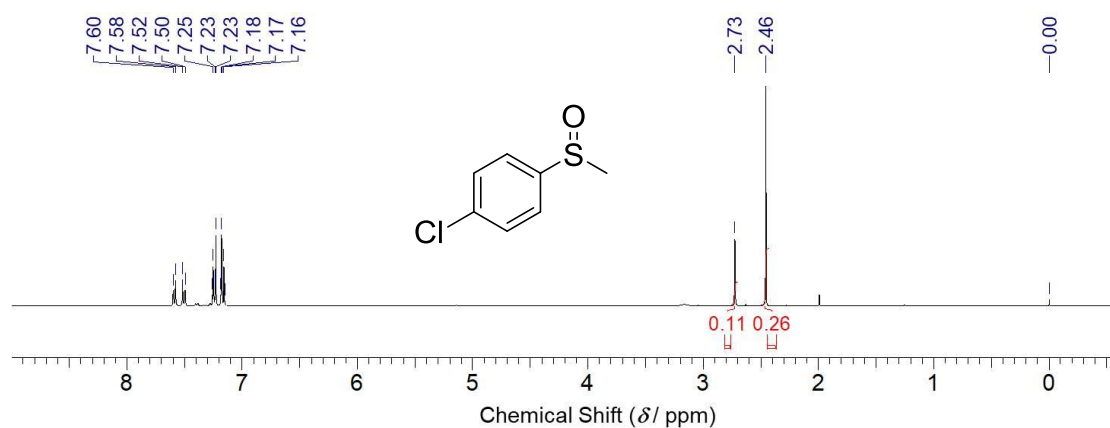

Figure S33. ^{1}H NMR (400Hz, CDCl$_3$). **RFTA** (0.5 mol %) as photocatalyst, in MeCN/MeOH 9:1 mixture, reaction time 6 h 25 min. Yield: 55 %.

S17

Figure S34. ^{1}H NMR (400Hz, CDCl$_3$). **FL** (0.5 mol %) as photocatalyst, in MeCN/MeOH 9:1 mixture, reaction time 6 h 25 min. Yield: 36 %.

Figure S35. ^{1}H NMR (400Hz, CDCl$_3$). **NI** (0.5 mol %) as photocatalyst, in MeCN/MeOH 9:1 mixture, reaction time 6 h 25 min. Yield: 0 %.
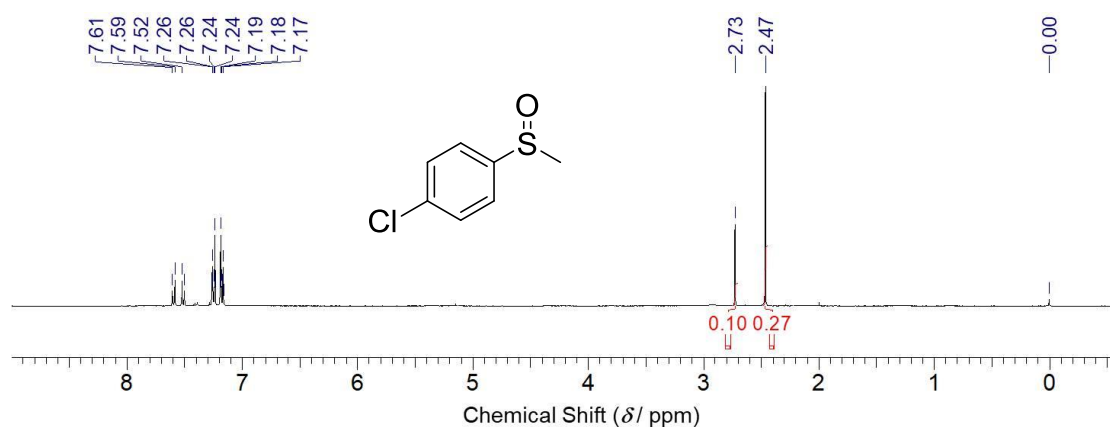

Figure S36. ^{1}H NMR (400Hz, CDCl$_3$). **NI-FL** (0.5 mol %) as photocatalyst, in MeCN/MeOH 9:1 mixture, reaction time 5 h 20 min. Yield: 89 %.

S18

Figure S37. ^{1}H NMR (400Hz, CDCl$_3$). **RFTA** (0.5 mol %) as photocatalyst, in MeCN/MeOH 9:1 mixture, reaction time 5 h 20 min. Yield: 79 %.

Figure S38. ^{1}H NMR (400Hz, CDCl$_3$). **FL** (0.5 mol %) as photocatalyst, in MeCN/MeOH 9:1 mixture, reaction time 5 h 20 min. Yield: 58 %.
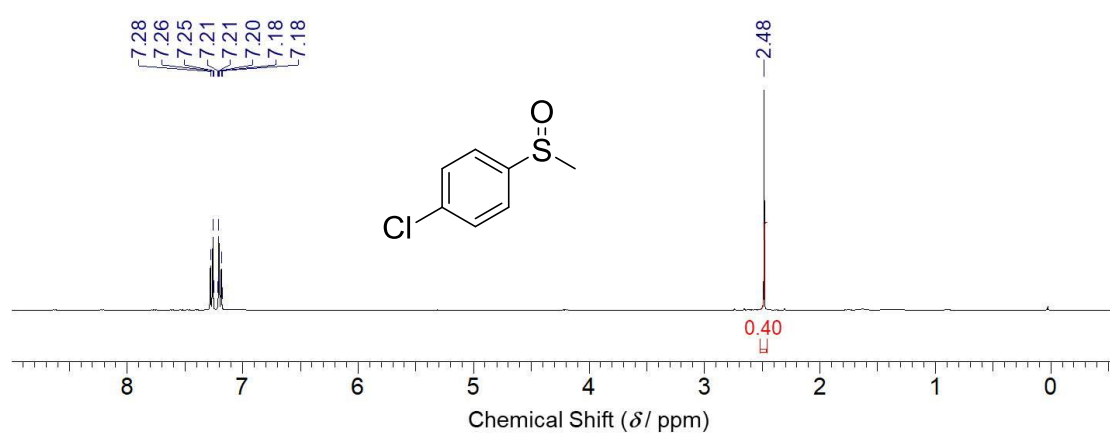

Figure S39. ^{1}H NMR (400Hz, CDCl$_3$). **NI** (0.5 mol %) as photocatalyst, in MeCN/MeOH 9:1 mixture, reaction time 5 h 20 min. Yield: 0 %.
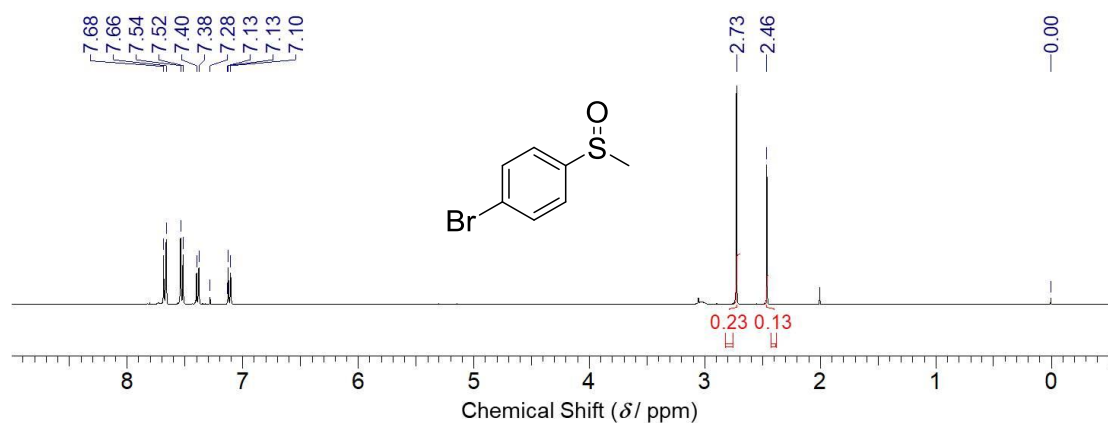
Figure S40. ^{1}H NMR (400Hz, CDCl$_3$). **NI-FL** (0.5 mol %) as photocatalyst, in MeCN/MeOH 9:1 mixture, reaction time 34 h. Yield: 35 %.
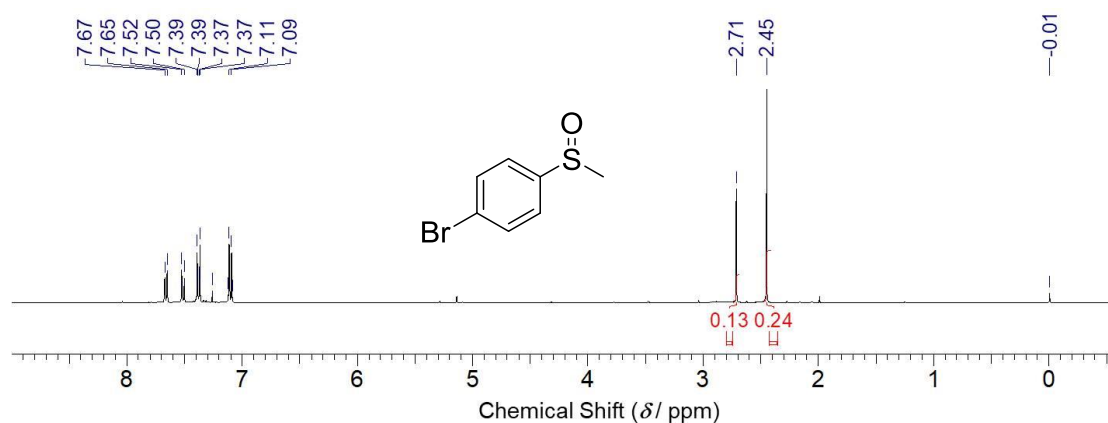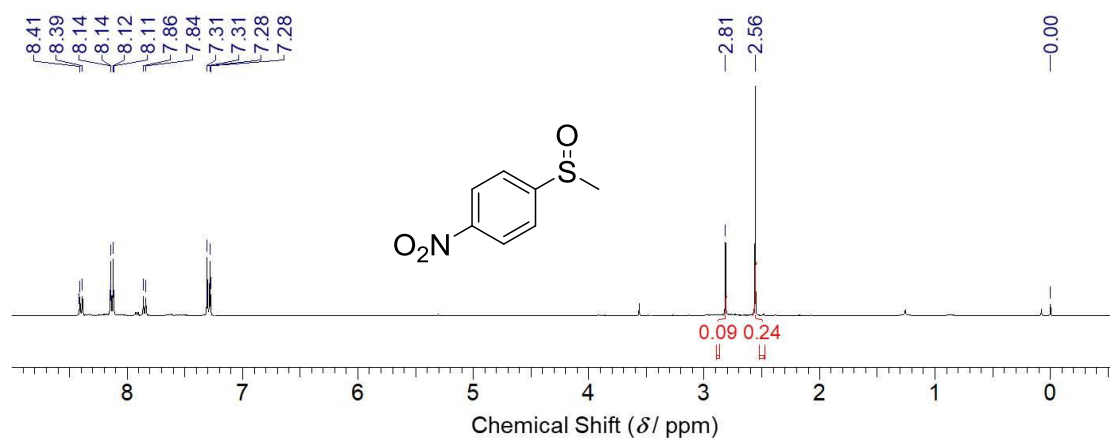

Figure S41. ^{1}H NMR (400Hz, CDCl$_3$). **RFTA** (0.5 mol %) as photocatalyst, in MeCN/MeOH 9:1 mixture, reaction time 34 h. Yield: 27 %.
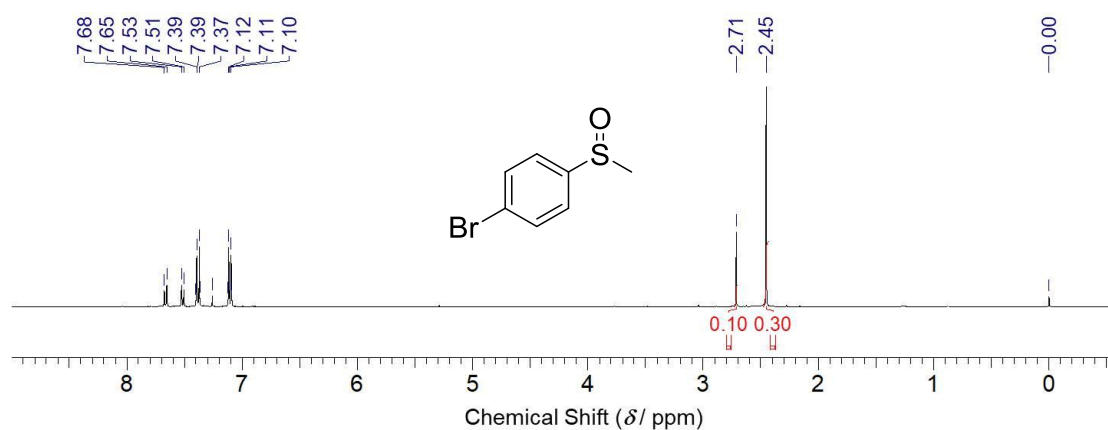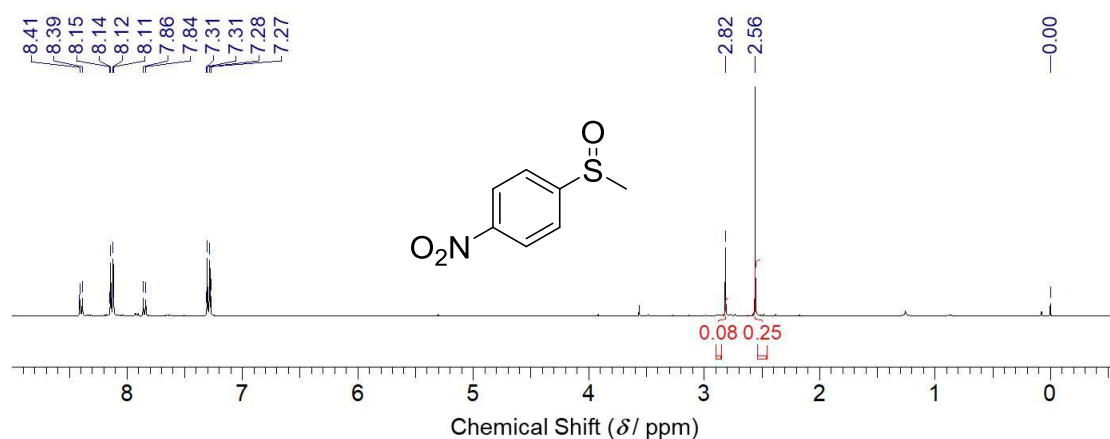

Figure S42. ^{1}H NMR (400Hz, CDCl$_3$). **FL** (0.5 mol %) as photocatalyst, in MeCN/MeOH 9:1 mixture, reaction time 34 h. Yield: 24 %.
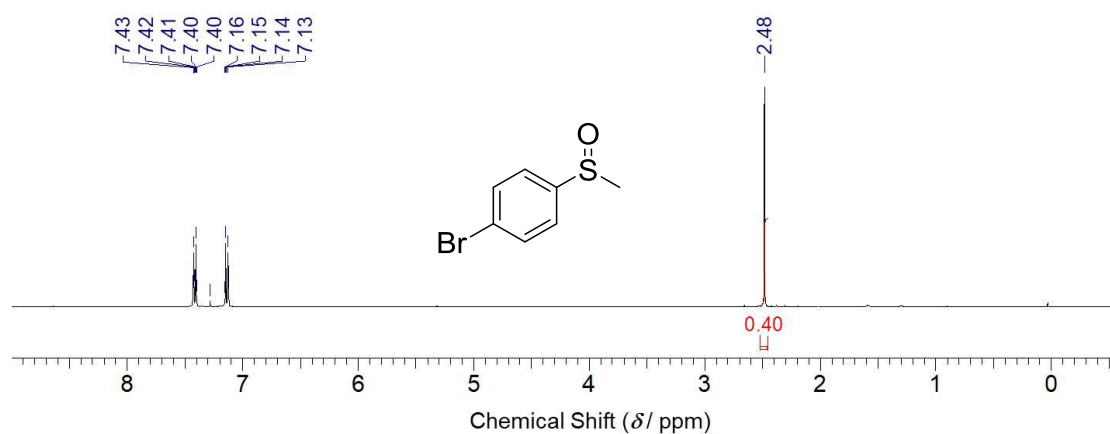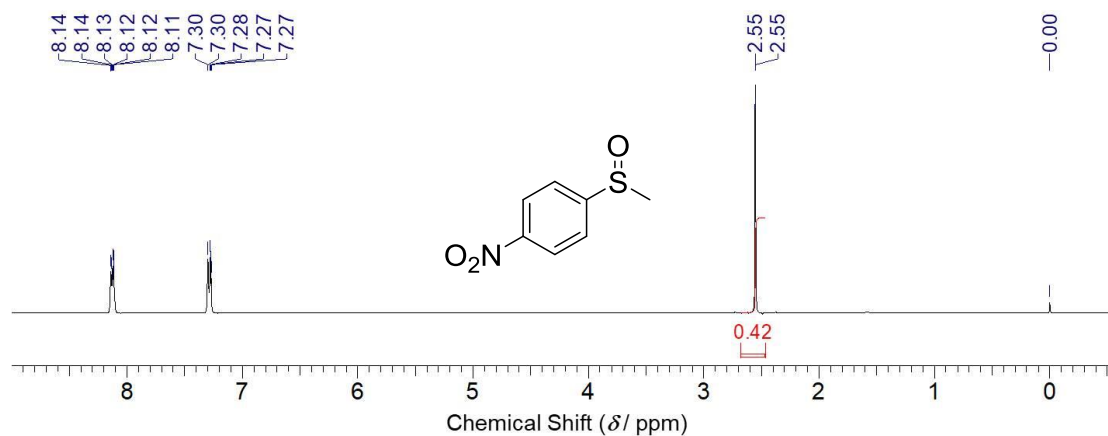
Figure S43. ^{1}H NMR (400Hz, CDCl$_3$). **NI** (0.5 mol %) as photocatalyst, in MeCN/MeOH 9:1 mixture, reaction time 34 h. Yield: 0 %.
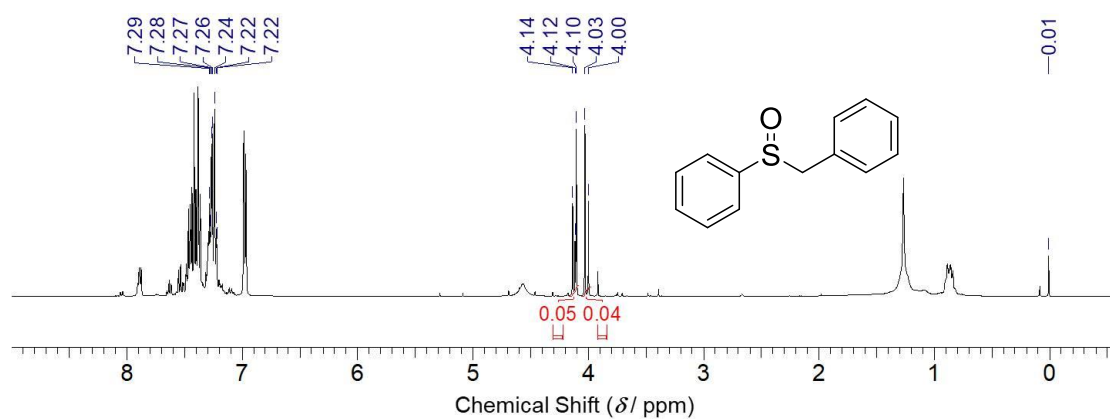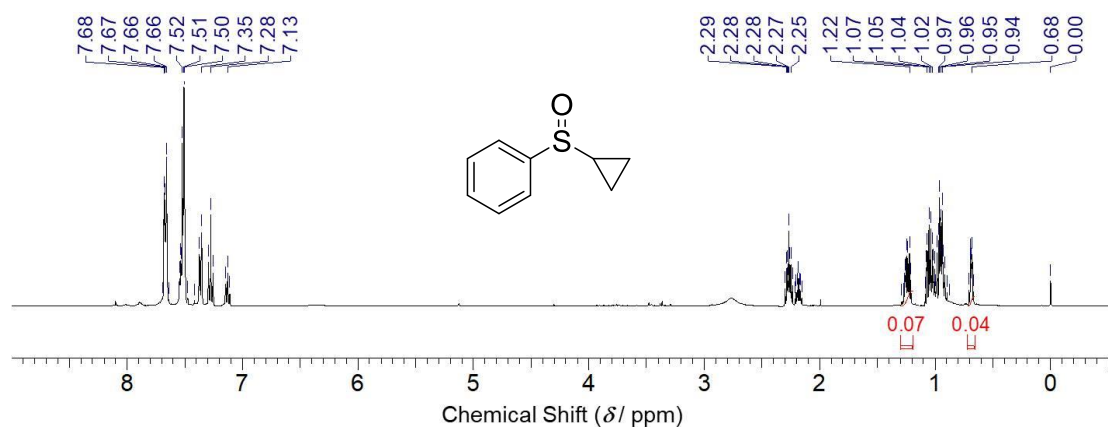

Figure S44. ^{1}H NMR (400Hz, CDCl$_3$). **NI-FL** (0.5 mol %) as photocatalyst, in MeCN/MeOH 9:1 mixture, reaction time 16 h 35 min. Yield: 64 %.
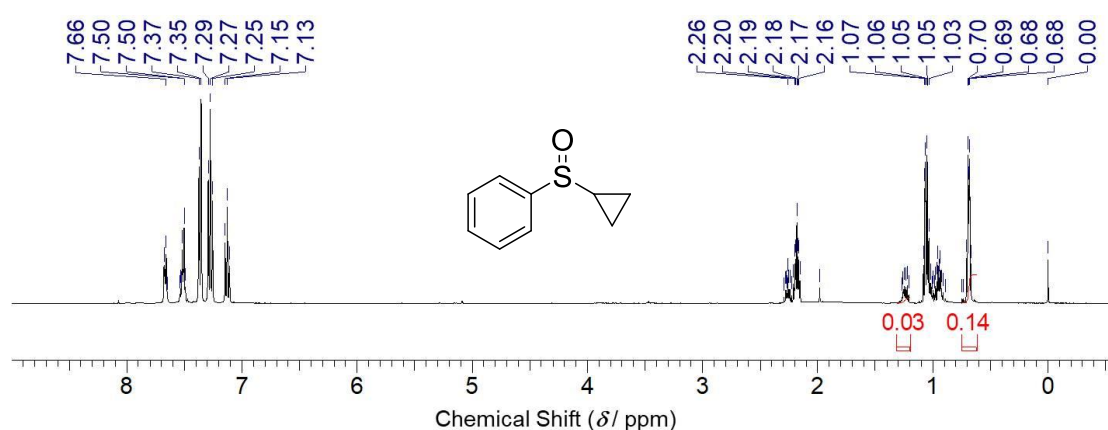
Figure S45. ^{1}H NMR (400Hz, CDCl$_3$). **RFTA** (0.5 mol %) as photocatalyst, in MeCN/MeOH 9:1 mixture, reaction time 16 h 35 min. Yield: 18 %.

S21
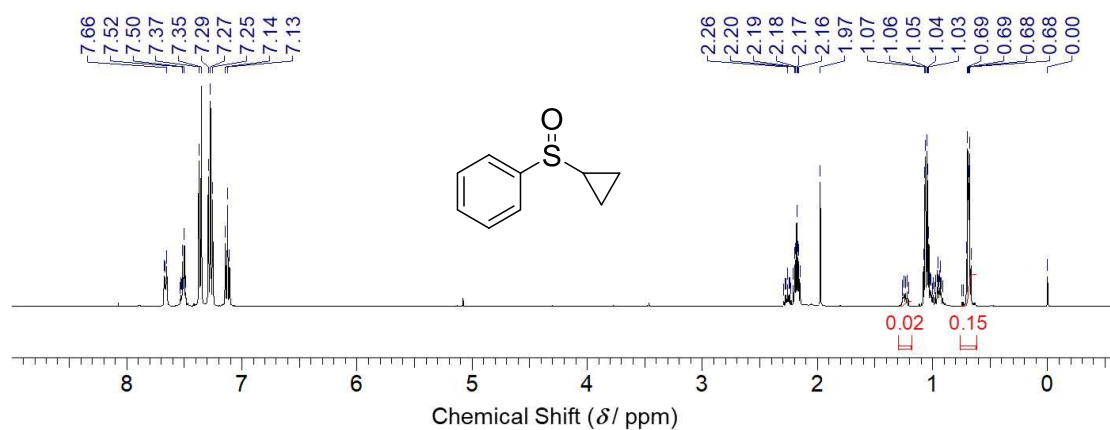
Figure S46. ^{1}H NMR (400Hz, CDCl$_3$). **FL** (0.5 mol %) as photocatalyst, in MeCN/MeOH 9:1 mixture, reaction time 16 h 35 min. Yield: 12 %.
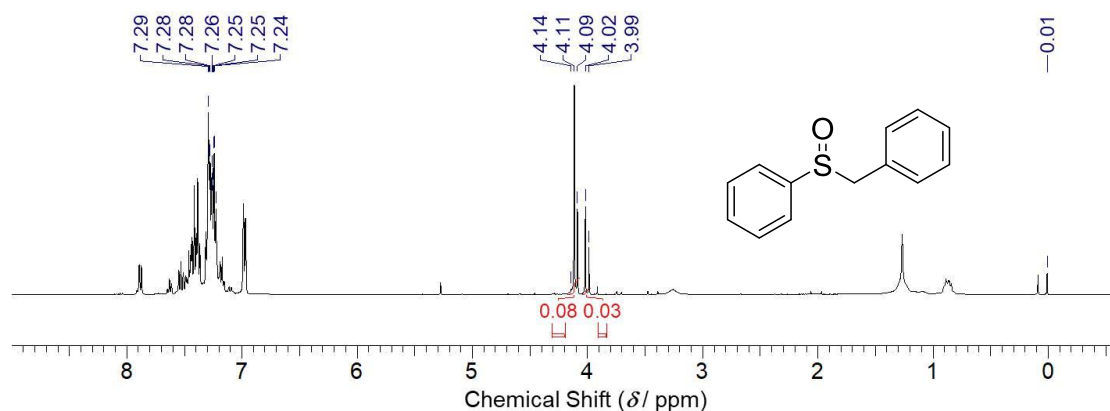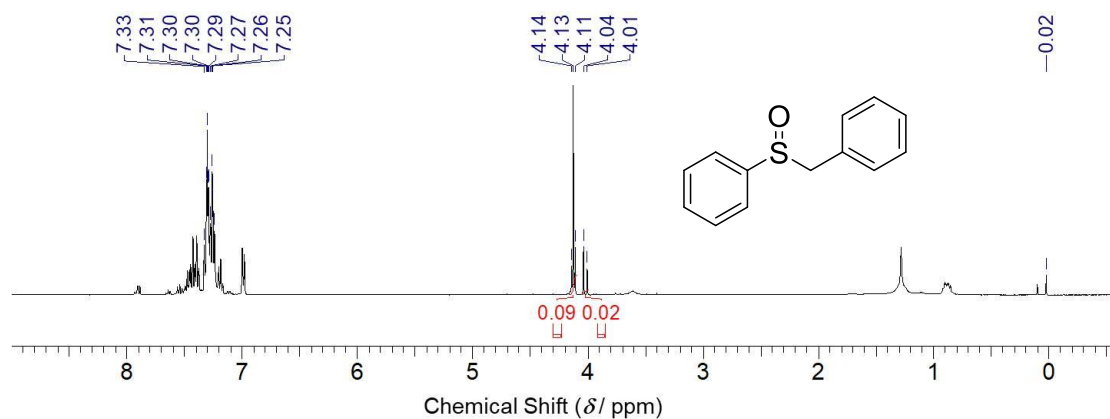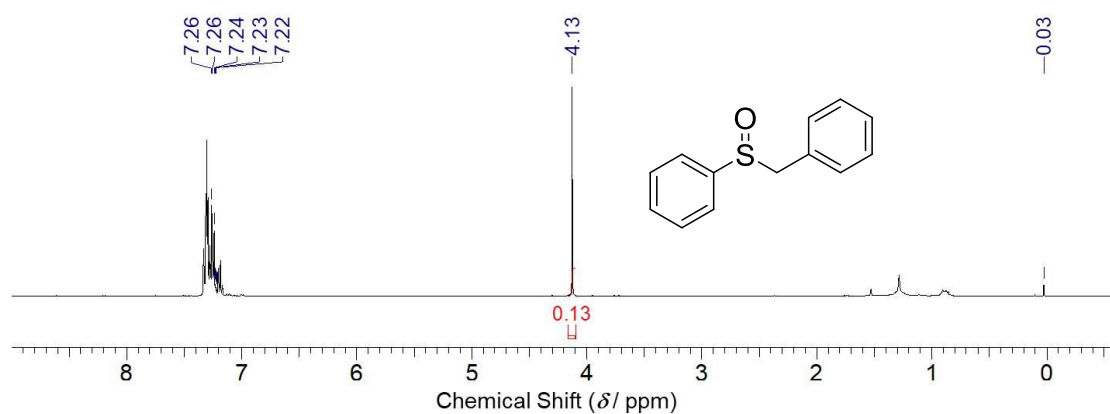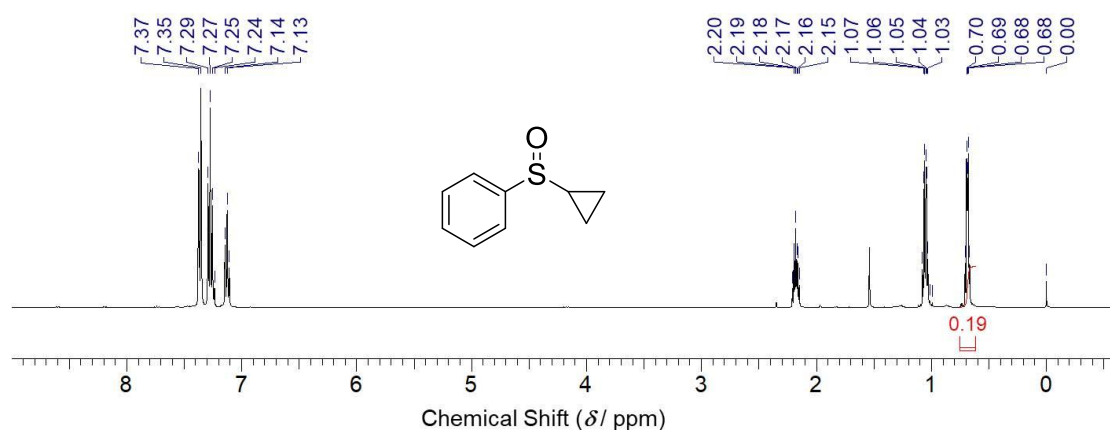

Figure S47. ^{1}H NMR (400Hz, CDCl$_3$). **NI** (0.5 mol %) as photocatalyst, in MeCN/MeOH 9:1 mixture, reaction time 16 h 35 min. Yield: 0 %.
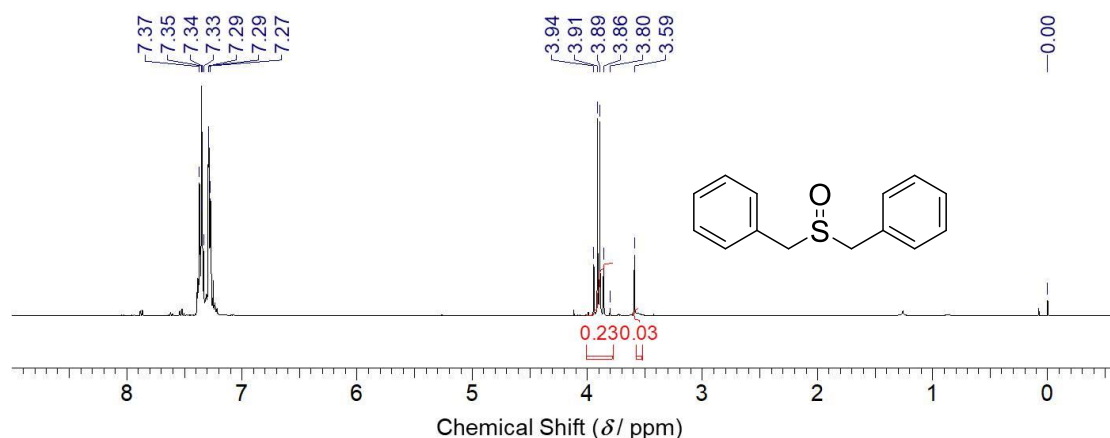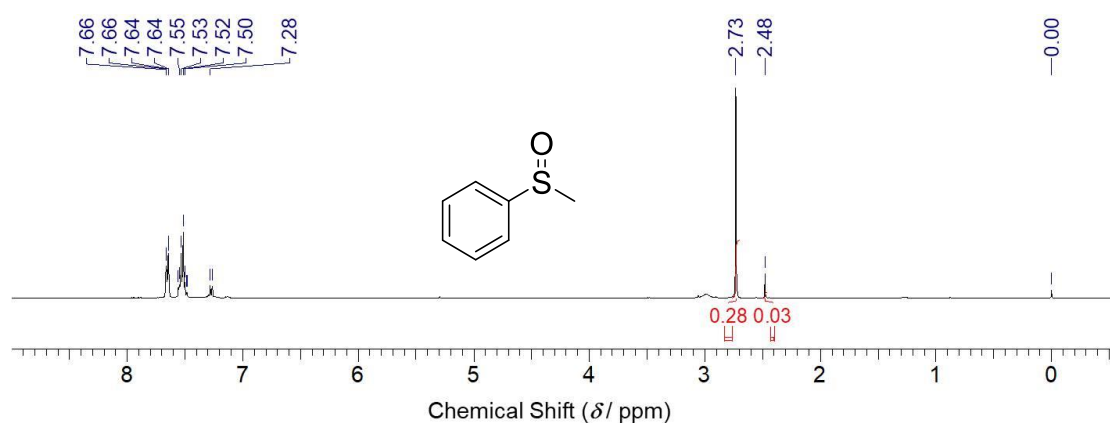

Figure S48. ^{1}H NMR (400Hz, CDCl$_3$). **NI-FL** (0.5 mol %) as photocatalyst, in MeCN/MeOH 9:1 mixture, reaction time 9 h, with 5 mol % DABCO. Yield: 90 %.
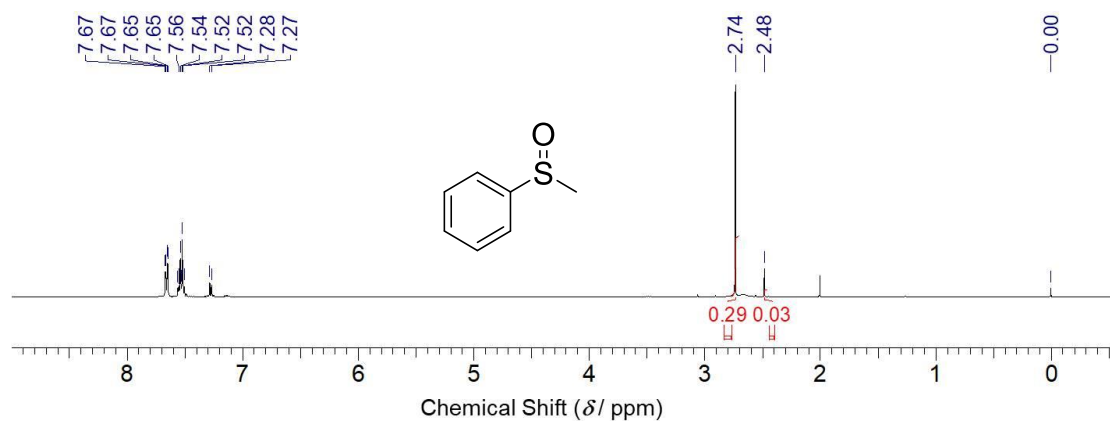
Figure S49. ^{1}H NMR (400Hz, CDCl$_3$). **NI-FL** (0.5 mol %) as photocatalyst, in MeCN/MeOH 9:1 mixture, reaction time 9 h, with 5 mol % BQ. Yield: 91 %.
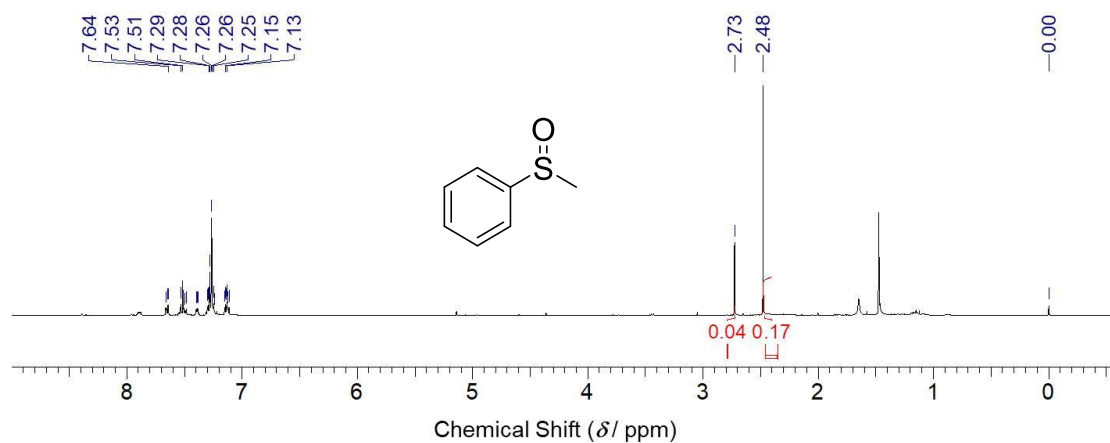
Figure S50. ^{1}H NMR (400Hz, CDCl$_3$). **NI-FL** (0.5 mol %) as photocatalyst, in MeCN/MeOH 9:1 mixture, reaction time 9 h, with 15 mol % TEMPO. Yield: 19 %.
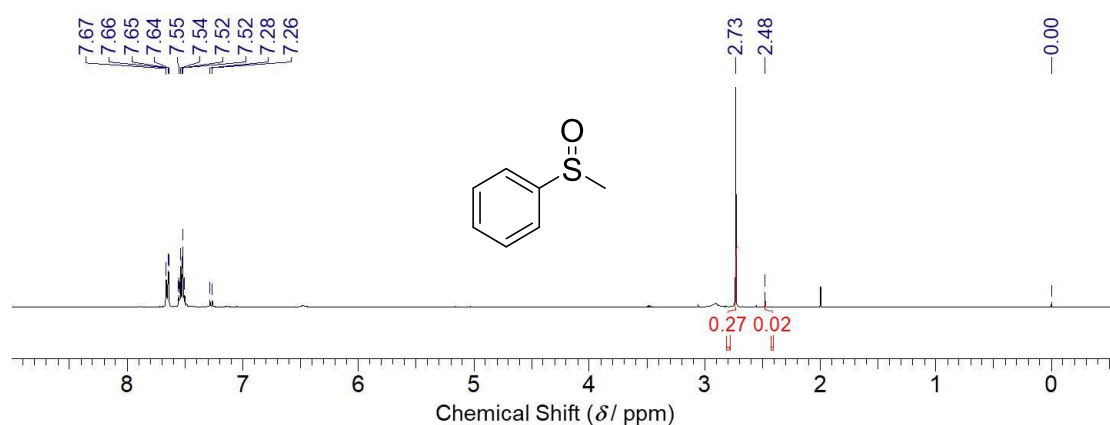
Figure S51. ^{1}H NMR (400Hz, CDCl$_3$). **NI-FL** (0.5 mol %) as photocatalyst, in MeCN/MeOH 9:1 mixture, reaction time 9 h, with 3 mol % MB. Yield: 93 %.
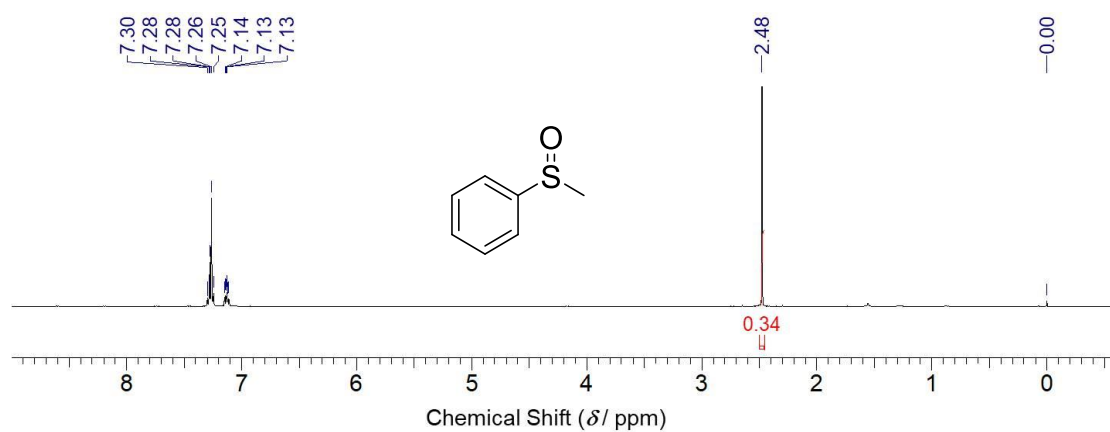
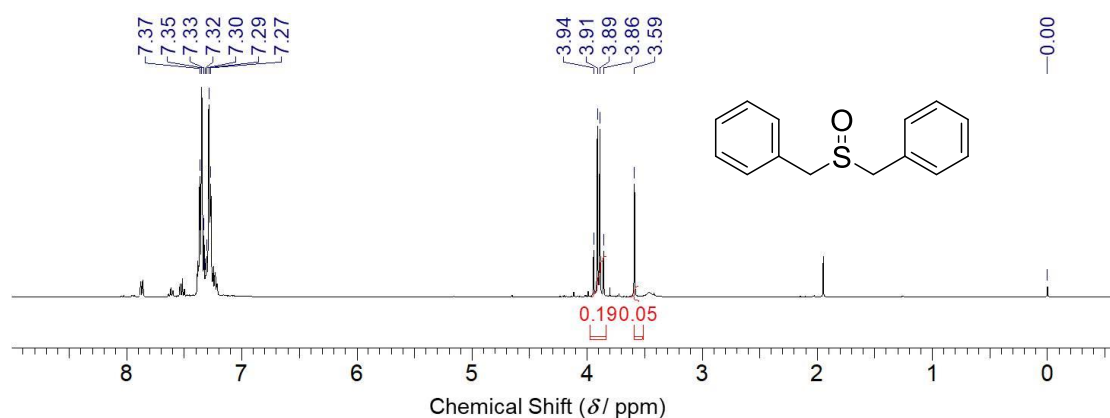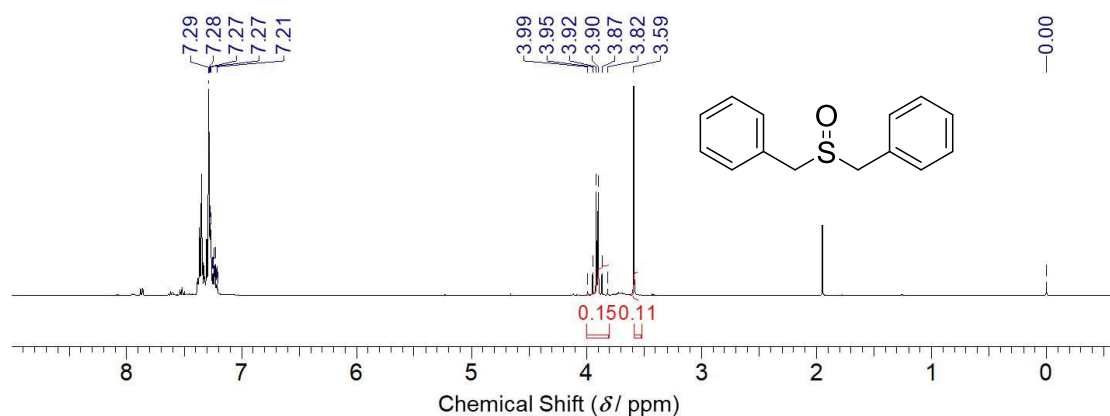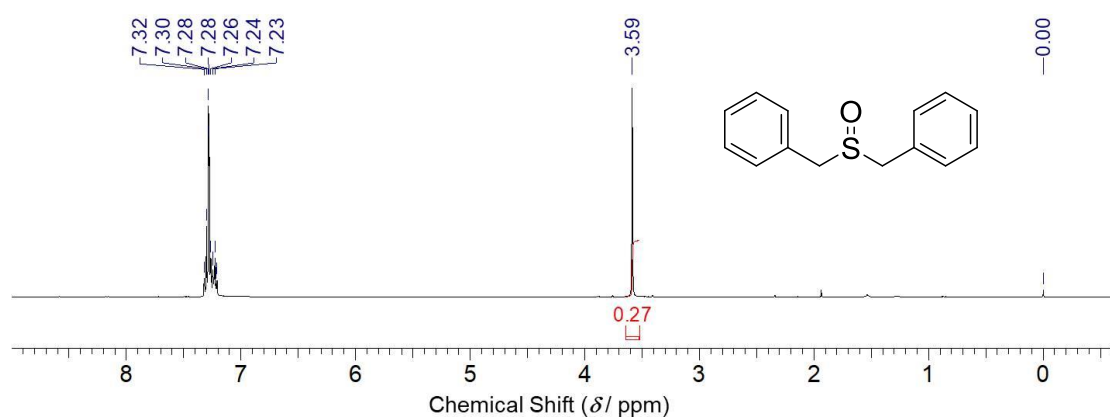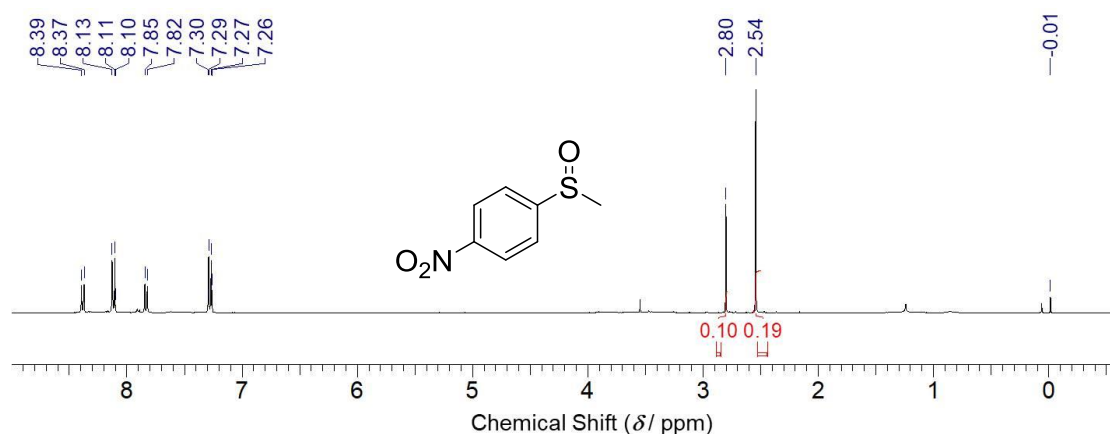**Figure S52.** ^{1}H NMR (400Hz, CDCl$_3$). **NI-FL** (0.5 mol %) as photocatalyst, in MeCN/MeOH 9:1 mixture, reaction time 9 h(no light), with 3 mol % MB. Yield: 0 %.

4 DFT/TD-DFT Results

Theoretical Methods

The electronic structure and photophysical properties of these sensitizers were investigated with Density Functional Theory (DFT) and Time-dependent (TD)-DFT based calculations. The alkyl groups in chromophores were simplified to $-CH_3$. S_0 structures of sensitizers were fully optimized with 6-311G(d) basis sets[5-7] and B3LYP functional.[8-9] The impact of potential interactions with solvents to electronic structure of sensitizers were treated with Polarizable Continuum Model (PCM).[10-12] Sensitizers at S_1 and T_n were obtained with TD-DFT calculations based on the S_0 structures. These calculations were performed with Gaussian 16.[13] The T_n to S_0 transition dipole moments were evaluated with quadratic response function[14-16] and the spin−orbit coupling constants were calculated with Dalton with effective single electron approximation in linear response theory.[17-19] With the electronic structure of sensitizers at S_0 and excited states, photophysical properties of NI-FL and FL were investigated within the Thermal Vibration Correlation Function (TVCF) formalism as implemented in MOMAP.[20-24]

Table S1. Electronic transitions involved in the excitation of NI-FL.

	Energy	f	Composition	CI	Character
$S_0{\rightarrow}S_1$	2.8109 eV / 441.09 nm	0.2475	93 → 94	0.69736	$\pi{\rightarrow}\pi^*$ $n{\rightarrow}\pi^*$
$S_0{\rightarrow}S_2$	3.2491 eV / 381.60 nm	0.2485	92 → 94	0.22538	$\pi{\rightarrow}\pi^*$
			93 → 95	0.65609	$n{\rightarrow}\pi^*$
$S_0{\rightarrow}S_3$	3.3012 eV / 375.57 nm	0.0077	89 → 94	0.36696	$\pi{\rightarrow}\pi^*$
			91 → 94	0.56186	$n{\rightarrow}\pi^*$
$S_0{\rightarrow}S_4$	3.4410 eV / 360.32 nm	0.0016	89 → 94	0.55988	$\pi{\rightarrow}\pi^*$
			91 → 94	0.38530	$n{\rightarrow}\pi^*$
$S_0{\rightarrow}S_5$	3.6572 eV / 339.02 nm	0.5674	87 → 94	0.11266	$\pi{\rightarrow}\pi^*$ $n{\rightarrow}\pi^*$
			92 → 94	0.63229	$n{\rightarrow}\pi^*$
			92 → 95	0.13999	$\pi{\rightarrow}\pi^*$
			93 → 95	0.21562	$\pi{\rightarrow}\pi^*$ $n{\rightarrow}\pi^*$
$S_0{\rightarrow}S_6$	3.8173 eV / 324.80 nm	0.0002	90 → 94	0.24994	$\pi{\rightarrow}\pi^*$
			90 → 95	0.62707	$n{\rightarrow}\pi^*$
$S_0{\rightarrow}S_7$	3.8908 eV / 318.66 nm	0.0025	90 → 94	0.64277	$\pi{\rightarrow}\pi^*$
			90 → 95	0.25579	$n{\rightarrow}\pi^*$
$S_0{\rightarrow}S_8$	3.9671 eV / 312.53 nm	0.0428	87 → 94	0.31043	$\pi{\rightarrow}\pi^*$
			88 → 94	0.33418	$n{\rightarrow}\pi^*$
			92 → 94	0.15968	
			92 → 95	0.47040	
$S_0{\rightarrow}S_9$	4.0510 eV / 306.06 nm	0.0852	86 → 94	0.12564	$\pi{\rightarrow}\pi^*$
			88 → 94	0.56027	$n{\rightarrow}\pi^*$
			88 → 95	0.10110	
			92 → 95	0.34107	
			93 → 97	0.11093	
$S_0{\rightarrow}S_{10}$	4.0811 eV / 303.80 nm	0.0002	84 → 94	0.57677	$\pi{\rightarrow}\pi^*$
			85 → 94	0.22201	$n{\rightarrow}\pi^*$
			91 → 95	0.27877	
$S_0{\rightarrow}T_1$	2.0312 eV / 610.38 nm	0	92 → 94	0.13332	$\pi{\rightarrow}\pi^*$
			93 → 94	0.68014	$n{\rightarrow}\pi^*$
$S_0{\rightarrow}T_2$	2.3531 eV / 526.89 nm	0	92 → 95	0.12950	$\pi{\rightarrow}\pi^*$
			93 → 95	0.64670	$n{\rightarrow}\pi^*$
$S_0{\rightarrow}T_3$	2.8775 eV / 430.87 nm	0	82 → 94	0.17580	$\pi{\rightarrow}\pi^*$
			89 → 94	0.55492	$n{\rightarrow}\pi^*$
			91 → 94	0.33467	
$S_0{\rightarrow}T_4$	3.0034 eV / 412.81 nm	0	88 → 94	0.17935	$\pi{\rightarrow}\pi^*$
			92 → 94	0.62248	$n{\rightarrow}\pi^*$
			93 → 94	0.12647	
			93 → 95	0.14506	
$S_0{\rightarrow}T_5$	3.2010 eV / 387.33 nm	0	84 → 94	0.15747	$\pi{\rightarrow}\pi^*$
			89 → 94	0.31687	$n{\rightarrow}\pi^*$
			91 → 94	0.57998	

Table S2. Electronic transitions involved in the excitation of FL.

	Energy	f	Composition	CI	Character
$S_0 \to S_1$	3.0228 eV / 410.17 nm	0.2154	$59 \to 60$	0.69596	$\pi \to \pi^* \ n \to \pi^*$
$S_0 \to S_2$	3.3213 eV / 373.30 nm	0.0008	$56 \to 60$	0.50648	$\pi \to \pi^* \ n \to \pi^*$
			$57 \to 60$	0.48128	
$S_0 \to S_3$	3.4578 eV / 358.56 nm	0.0077	$54 \to 60$	0.11506	$\pi \to \pi^* \ n \to \pi^*$
			$56 \to 60$	0.48043	
			$57 \to 60$	0.49591	
$S_0 \to S_4$	3.7653 eV / 329.28 nm	0.1849	$58 \to 60$	0.68106	$\pi \to \pi^*$
			$59 \to 61$	0.14574	
$S_0 \to S_5$	4.1396 eV / 299.51 nm	0.0000	$54 \to 60$	0.68088	$\pi \to \pi^*$
			$57 \to 60$	0.11784	
$S_0 \to S_6$	4.2086 eV / 294.60 nm	0.0121	$55 \to 60$	0.68290	$\pi \to \pi^*$
			$59 \to 61$	0.13615	
$S_0 \to S_7$	4.6710 eV / 265.43 nm	0.0004	$52 \to 60$	0.68355	$\pi \to \pi^*$
			$56 \to 61$	0.13184	
$S_0 \to S_8$	4.8351 eV / 256.43 nm	0.0411	$53 \to 60$	0.64915	$\pi \to \pi^*$
			$58 \to 61$	0.23567	
$S_0 \to S_9$	4.8868 eV / 253.71 nm	0.7330	$55 \to 60$	0.15106	$\pi \to \pi^*$
			$58 \to 60$	0.11486	
			$59 \to 61$	0.65720	
$S_0 \to S_{10}$	5.2127 eV / 237.85 nm	0.0003	$52 \to 60$	0.12308	$\pi \to \pi^*$
			$56 \to 61$	0.59583	
			$57 \to 61$	0.33929	
$S_0 \to T_1$	2.1525 eV / 575.99 nm	0	$58 \to 60$	0.10500	$\pi \to \pi^*$
			$59 \to 60$	0.69492	
$S_0 \to T_2$	2.7569 eV / 449.73 nm	0	$58 \to 60$	0.65690	$\pi \to \pi^*$
			$58 \to 62$	0.14226	
			$59 \to 60$	0.10178	
			$59 \to 61$	0.13928	
$S_0 \to T_3$	2.8738 eV / 431.42 nm	0	$52 \to 60$	0.20068	$\pi \to \pi^*$
			$56 \to 60$	0.59672	
			$57 \to 60$	0.29532	
$S_0 \to T_4$	3.2394 eV / 382.74 nm	0	$54 \to 60$	0.17157	$\pi \to \pi^*$
			$56 \to 60$	0.28110	
			$57 \to 60$	0.60386	
			$93 \to 95$	0.14506	
$S_0 \to T_5$	3.5830 eV / 346.04 nm	0	$55 \to 60$	0.60977	$\pi \to \pi^*$
			$55 \to 63$	0.12513	
			$58 \to 60$	0.11352	
			$59 \to 61$	0.28154	

Table S3. Electronic transitions involved in the excitation of NI.

	Energy	f	Composition	CI	Character
$S_0 \rightarrow S_1$	3.6722 eV/ 337.63 nm	0.2428	55 → 56	0.69890	$\pi \rightarrow \pi^*$
$S_0 \rightarrow S_2$	3.8712 eV / 320.28 nm	0.0004	53 → 56	0.69357	$\pi \rightarrow \pi^*$
$S_0 \rightarrow S_3$	4.0066 eV / 309.45 nm	0.0326	54 → 56	0.65514	$\pi \rightarrow \pi^*$
			55 → 57	0.23330	
$S_0 \rightarrow S_4$	4.3062eV / 287.92 nm	0.0180	51 → 56	0.50108	$\pi \rightarrow \pi^*$
			52 → 56	0.45057	
			53 → 58	0.13601	
			55 → 57	0.13182	
$S_0 \rightarrow S_5$	4.5001 eV / 275.52 nm	0.0316	51 → 56	0.45599	$\pi \rightarrow \pi^*$
			52 → 56	0.46938	
			55 → 57	0.21893	
$S_0 \rightarrow S_6$	4.9235 eV / 251.82 nm	0.0021	50 → 56	0.42150	$\pi \rightarrow \pi^*$
			55 → 58	0.56502	
$S_0 \rightarrow S_7$	5.3249 eV / 232.84 nm	0.2870	50 → 56	0.42814	$\pi \rightarrow \pi^*$
			52 → 56	0.22430	
			52 → 59	0.10999	
			55 → 57	0.37585	
			55 → 58	0.28524	
$S_0 \rightarrow S_8$	5.4356 eV / 228.09 nm	0.4265	50 → 56	0.33697	$\pi \rightarrow \pi^*$
			52 → 56	0.11188	
			54 → 56	0.23641	
			54 → 59	0.15656	
			55 → 57	0.45830	
			55 → 58	0.28082	
$S_0 \rightarrow S_9$	5.5710 eV / 222.55 nm	0.0001	51 → 56	0.15945	$\pi \rightarrow \pi^*$
			53 → 57	0.14723	
			53 → 58	0.65529	
$S_0 \rightarrow S_{10}$	5.6331 eV / 220.10 nm	0.0002	50 → 57	0.20059	$\pi \rightarrow \pi^*$
			52 → 57	0.12574	
			54 → 58	0.65397	
$S_0 \rightarrow T_1$	2.3461 eV / 528.48 nm	0	50 → 58	0.11756	$\pi \rightarrow \pi^*$
			54 → 57	0.10968	
			55 → 56	0.68764	
$S_0 \rightarrow T_2$	3.3463 eV / 370.52 nm	0	50 → 56	0.12058	$\pi \rightarrow \pi^*$
			54 → 56	0.67352	
			55 → 58	0.12353	
$S_0 \rightarrow T_3$	3.5957 eV / 344.81 nm	0	51 → 58	0.12763	$\pi \rightarrow \pi^*$
			53 → 56	0.67633	
			53 → 59	0.14160	
$S_0 \rightarrow T_4$	3.7843 eV / 327.63 nm	0	50 → 56	0.42541	$\pi \rightarrow \pi^*$
			52 → 56	0.31310	
			54 → 56	0.12138	

			55 → 58	0.41610	
$S_0 \rightarrow T_5$	3.8041 eV / 325.93 nm	0	50 → 56	0.20816	$\pi \rightarrow \pi^*$
			52 → 56	0.59988	
			54 → 56	0.13039	
			55 → 58	0.21661	

5 Measurement of singlet oxygen quantum yield
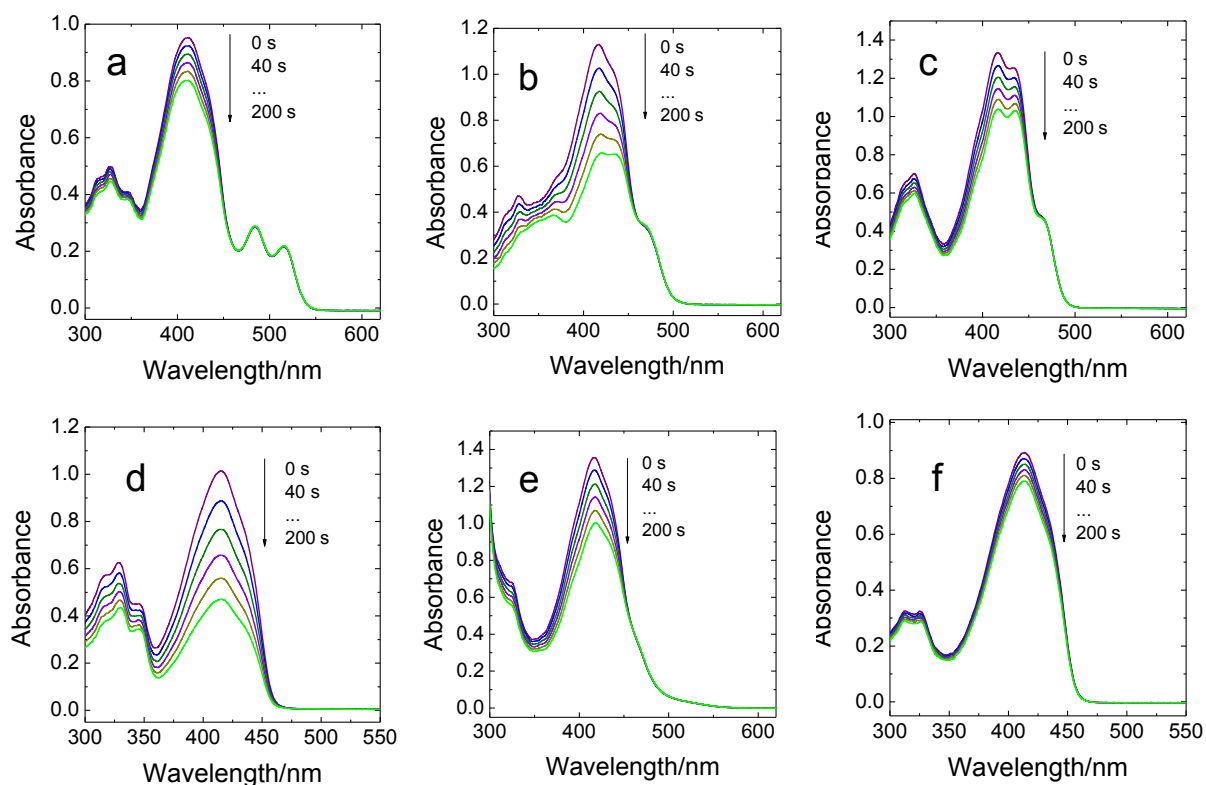
Figure S53. Absorption spectra of mixtures of unknown samples, namely NI-FL(a), RFTA(b), FL(c), NI(d), $[Ru(bpy)_3]^{2+}$(e) and none(f) with DPBF at different time. $[Ru(bpy)_3]^{2+}$ was used as standard ($\Phi_\Delta = 0.57$ in DCM); $\lambda_{ex} = 350$ nm, in toluene. 20 ℃.
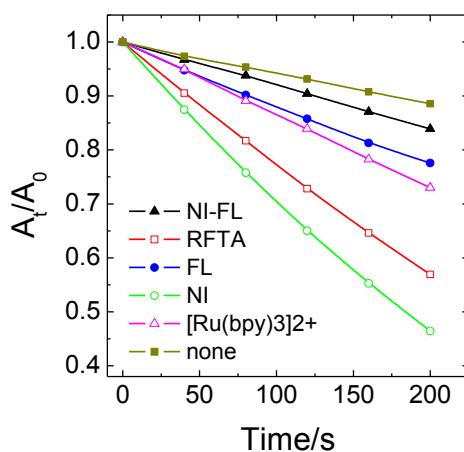
Figure S54. Changes of relative absorbance of DPBF+sample mixture at 414 nm with time, with NI-FL, RFTA, FL, NI, $[Ru(bpy)_3]^{2+}$ and none as samples. $[Ru(bpy)_3]^{2+}$ was used as standard ($\Phi_\Delta = 0.57$ in DCM); $\lambda_{ex} = 350$ nm, in toluene. 20 ℃. The fitted absolute values of slopes of NI-FL, RFTA, FL, NI, $[Ru(bpy)_3]^{2+}$ and none are 0.8×10^{-3}, 2.4×10^{-3}, 1.5×10^{-3}, 2.7×10^{-3}, 1.3×10^{-3} and 0.5×10^{-3} s^{-1}, respectively.

6 References

(1) Guo, H.; Zhu, L.; Dang, C.; Zhao, J.; Dick, B. Synthesis and photophysical properties of ruthenium(II) polyimine complexes decorated with flavin. *Phys. Chem. Chem. Phys.* **2018,** *20*, 17504-17516.

(2) Urban, M.; Durka, K.; Jankowski, P.; Serwatowski, J.; Lulinski, S. Highly Fluorescent Red-Light Emitting Bis(boranils) Based on Naphthalene Backbone. *J. Org. Chem.* **2017,** *82*, 8234-8241.

(3) Brouwer, A. M. Standards for photoluminescence quantum yield measurements in solution (IUPAC Technical Report). *Pure Appl. Chem.* **2011,** *83*, 2213-2228.

(4) Ishida, H.; Bunzli, J. C.; Beeby, A. Guidelines for measurement of luminescence spectra and quantum yields of inorganic and organometallic compounds in solution and solid state (IUPAC Technical Report). *Pure Appl. Chem.* **2016,** *88*, 701-711.

(5) Binning, R. C.; Curtiss, L. A. Compact Contracted Basis-sets for 3rd-row atoms - Ga- Kr. *J. Comput. Chem.* **1990,** *11*, 1206-1216.

(6) Francl, M. M.; Pietro, W. J.; Hehre, W. J.; Binkley, J. S.; Gordon, M. S.; Defrees, D. J.; Pople, J. A. Self-consistent Molecular-orbital Methods 23. A Polarization-type Basis Set for 2nd-row Elements. *J. Chem. Phys.* **1982,** *77*, 3654-3665.

(7) Rassolov, V. A.; Ratner, M. A.; Pople, J. A.; Redfern, P. C.; Curtiss, L. A. 6-31G*basis set for third-row atoms. *J. Comput. Chem.* **2001,** *22*, 976-984.

(8) Becke, A. D. Density-functional Thermochemistry 3. The role of exact exchange. *J. Chem. Phys.* **1993,** *98*, 5648-5652.

(9) Lee, C. T.; Yang, W. T.; Parr, R. G. Development of the Colle-Salvetti Correlations-energy Formula into a Functional of the Electron-density. *Phys. Rev. B* **1988,** *37*, 785-789.

(10) Miertus, S.; Scrocco, E.; Tomasi, J. Electrostatic Interaction of a Solute with a Continuum - A Direct Utilization of Abinitio Molecular Potentials for the Prevision of Solvent Effects. *Chem. Phys.* **1981,** *55*, 117-129.

(11) Cammi, R.; Mennucci, B. Linear response theory for the polarizable continuum model. *J. Chem. Phys.* **1999,** *110*, 9877-9886.

(12) Tomasi, J.; Mennucci, B.; Cammi, R. Quantum mechanical continuum solvation models. *Chem. Rev.* **2005,** *105*, 2999-3093.

(13) Frisch, M. J.; Trucks, G. W.; Schlegel, H. B.; Scuseria, G. E.; Robb, M. A.; Cheeseman, J. R.; Scalmani, G.; Barone, V.; Petersson, G. A.; Nakatsuji, H.; Li, X.; Caricato, M.; Marenich, A. V.; Bloino, J.; Janesko, B. G.; Gomperts, R.; Mennucci, B.; Hratchian, H. P.; Ortiz, J. V.; Izmaylov, A. F.; Sonnenberg, J. L.; Williams; Ding, F.; Lipparini, F.; Egidi, F.; Goings, J.; Peng, B.; Petrone, A.; Henderson, T.; Ranasinghe, D.; Zakrzewski, V. G.; Gao, J.; Rega, N.; Zheng, G.; Liang, W.; Hada, M.; Ehara, M.; Toyota, K.; Fukuda, R.; Hasegawa, J.; Ishida, M.; Nakajima, T.; Honda, Y.; Kitao, O.; Nakai, H.; Vreven, T.; Throssell, K.; Montgomery Jr., J. A.; Peralta, J. E.; Ogliaro, F.; Bearpark, M. J.; Heyd, J. J.; Brothers, E. N.; Kudin, K. N.; Staroverov, V. N.; Keith, T. A.; Kobayashi, R.; Normand, J.; Raghavachari, K.; Rendell, A. P.; Burant, J. C.; Iyengar, S. S.; Tomasi, J.; Cossi, M.; Millam, J. M.; Klene, M.; Adamo, C.; Cammi, R.; Ochterski, J. W.; Martin, R. L.; Morokuma, K.; Farkas, O.; Foresman, J. B.; Fox, D. J. *Gaussian 16 Rev. A.03*, Wallingford, CT, 2016.

(14) Vahtras, O.; Agren, H.; Jorgensen, P.; Jensen, H. J. A.; Helgaker, T.; Olsen, J. Multiconfigurational Quadratic Response Functions for Singlet and Triplet Perturbations- The

Phosphorescence Lifetime of Formaldehyde. *J. Chem. Phys.* **1992,** *97*, 9178-9187.

(15) Hettema, H.; Jensen, H. J. A.; Jorgensen, P.; Olsen, J. Quadratic Response Functions for a Multiconfigurational Self-consistent Field Wave-function. *J. Chem. Phys.* **1992,** *97*, 1174-1190.

(16) Agren, H.; Vahtras, O.; Koch, H.; Jorgensen, P.; Helgaker, T. Direct Atomic Orbital Based Self-consistent-field Calculations of Nonlinear Molecular-properties - Application to the Frequency-dependent Hyperpolarizability of Para-nitroaniline. *J. Chem. Phys.* **1993,** *98*, 6417-6423.

(17) Olsen, J.; Yeager, D. L.; Jorgensen, P. Triplet Excitation Properties in Large-scale Multiconfiguration Linear Response Calculations. *J. Chem. Phys.* **1989,** *91*, 381-388.

(18) Jorgensen, P.; Jensen, H. J. A.; Olsen, J. Linear Response Calculations for Large-scale Multiconfiguration Self-consistent Field Wave-functions. *J. Chem. Phys.* **1988,** *89*, 3654-3661.

(19) Aidas, K.; Angeli, C.; Bak, K. L.; Bakken, V.; Bast, R.; Boman, L.; Christiansen, O.; Cimiraglia, R.; Coriani, S.; Dahle, P.; Dalskov, E. K.; Ekstrom, U.; Enevoldsen, T.; Eriksen, J. J.; Ettenhuber, P.; Fernandez, B.; Ferrighi, L.; Fliegl, H.; Frediani, L.; Hald, K.; Halkier, A.; Hattig, C.; Heiberg, H.; Helgaker, T.; Hennum, A. C.; Hettema, H.; Hjertenaes, E.; Host, S.; Hoyvik, I. M.; Iozzi, M. F.; Jansik, B.; Jensen, H. J. A.; Jonsson, D.; Jorgensen, P.; Kauczor, J.; Kirpekar, S.; Kjrgaard, T.; Klopper, W.; Knecht, S.; Kobayashi, R.; Koch, H.; Kongsted, J.; Krapp, A.; Kristensen, K.; Ligabue, A.; Lutnaes, O. B.; Melo, J. I.; Mikkelsen, K. V.; Myhre, R. H.; Neiss, C.; Nielsen, C. B.; Norman, P.; Olsen, J.; Olsen, J. M. H.; Osted, A.; Packer, M. J.; Pawlowski, F.; Pedersen, T. B.; Provasi, P. F.; Reine, S.; Rinkevicius, Z.; Ruden, T. A.; Ruud, K.; Rybkin, V. V.; Salek, P.; Samson, C. C. M.; de Meras, A. S.; Saue, T.; Sauer, S. P. A.; Schimmelpfennig, B.; Sneskov, K.; Steindal, A. H.; Sylvester-Hvid, K. O.; Taylor, P. R.; Teale, A. M.; Tellgren, E. I.; Tew, D. P.; Thorvaldsen, A. J.; Thogersen, L.; Vahtras, O.; Watson, M. A.; Wilson, D. J. D.; Ziolkowski, M.; Agren, H. The Dalton quantum chemistry program system. *Wiley Interdiscip. Rev.-Comput. Mol. Sci.* **2014,** *4*, 269-284.

(20) Peng, Q.; Yi, Y. P.; Shuai, Z. G.; Shao, J. S. Excited state radiationless decay process with Duschinsky rotation effect: Formalism and implementation. *J. Chem. Phys.* **2007,** *126*, 114302.

(21) Peng, Q.; Yi, Y. P.; Shuai, Z. G.; Shao, J. S. Toward quantitative prediction of molecular fluorescence quantum efficiency: Role of Duschinsky rotation. *J. Am. Chem. Soc.* **2007,** *129*, 9333-9339.

(22) Niu, Y. L.; Peng, Q. A.; Deng, C. M.; Gao, X.; Shuai, Z. G. Theory of Excited State Decays and Optical Spectra: Application to Polyatomic Molecules. *J. Phys. Chem. A* **2010,** *114*, 7817-7831.

(23) Niu, Y.; Peng, Q.; Shuai, Z. Promoting-mode free formalism for excited state radiationless decay process with Duschinsky rotation effect. *Sci. China Ser. B-Chem.* **2008,** *51*, 1153-1158.

(24) Peng, Q.; Niu, Y. L.; Shi, Q. H.; Gao, X.; Shuai, Z. G. Correlation Function Formalism for Triplet Excited State Decay: Combined Spin-Orbit and Nonadiabatic Couplings. *J. Chem. Theory Comput.* **2013,** *9*, 1132-1143.